R. & M. No. 3145
(19,428)
A.R.C. Technical Report

MINISTRY OF AVIATION

AERONAUTICAL RESEARCH COUNCIL
REPORTS AND MEMORANDA

Wind-Tunnel Tests on the Use of Distributed Suction for Maintaining Laminar Flow on a Body of Revolution

By

N. GREGORY, M.A. and W. S. WALKER,
of the Aerodynamics Division, N.P.L.

LONDON: HER MAJESTY'S STATIONERY OFFICE
1960
PRICE 11*s*. 6*d*. NET

Wind-Tunnel Tests on the Use of Distributed Suction for Maintaining Laminar Flow on a Body of Revolution

By

N. GREGORY, M.A. and W. S. WALKER,
of the Aerodynamics Division, N.P.L.

Reports and Memoranda No. 3145*

July, 1957

Summary.—Experiments were carried out in the National Physical Laboratory 13-ft × 9-ft Wind Tunnel on a 15-ft long body of revolution of fineness ratio 10 : 1. Observations were made of the effects of Reynolds number, yaw, and of isolated excrescences on the position of transition on the solid body, and the possibilities of increasing the extent of laminar flow by means of area suction were examined.

At zero angle of yaw, the maximum Reynolds number at transition on a solid version of the body was $4\frac{1}{2}$ million. When the body was set at a small angle of yaw, the transition position was much farther forward along certain generators of the body than on others, owing to the instability of the three-dimensional boundary layer. The critical heights of small conical excrescences which just precipitated transition were found to be much the same as those required on a two-dimensional aerofoil.

The ' suction ' version of the body was porous over the central third of the length and was attached to the overhead tunnel balance by means of a porous wing. There appeared to be no fundamental difficulty in obtaining extended laminar flow over the body with distributed suction up to a tunnel speed of 80 ft/sec. Above this speed, the skin joints were too rough, and numerous wedges of turbulence originating from the joints spoiled the laminar flow. The adverse effects of yaw which were noticed on the solid body were not encountered and far-back transition was obtained with the same suction quantity as was needed at zero yaw. This suction quantity was large ($v_0/U_0 \doteq 0{\cdot}0009$ on the body), because of the rough surface.

The suction applied at the wing-body intersection (locally $v_0/U_0 \doteq 0{\cdot}003$) reduced the secondary flow in the boundary layer and enabled laminar flow to be maintained in this region at a wind speed of 80 ft/sec despite experimental difficulties over awkward skin joints. Even with laminar flow right round the intersection to the trailing edge of the wing, the laminar wake from the wing rapidly became turbulent downstream of the trailing edge and gave rise to a spreading wedge of turbulent boundary layer on the body. Further investigation of this difficulty would best be carried out on a simple part model, such as the junction of a stub wing with a flat plate.

Partly in consequence of the large suction quantity needed for laminar flow, and partly because the flow on the body in the wake of the wing and aft of 0·82 of the body length remained turbulent when suction was applied, there was only a small reduction in the effective drag coefficient of the model with suction. The analysis shows, however, that the potential gains at high Reynolds numbers would be large, provided the porous surface were satisfactorily smooth and extended sufficiently far back to enable full-length laminar flow to be achieved.

1. *Introduction.*—By the beginning of 1952, experiments carried out in the N.P.L. 13-ft × 9-ft Wind Tunnel had shown[1] that a laminar boundary layer could be maintained over the surface of a two-dimensional wing by suction through 14 spanwise porous strips. Transition was delayed to aft of the 0·9 chord position up to the top wind speed obtainable in the tunnel, 210 ft/sec (chord Reynolds number $1{\cdot}07 \times 10^7$), with considerable reduction in the effective drag coefficient. Work proceeding elsewhere had shown that boundary-layer control using multiple slots or wholly porous areas were equally satisfactory methods of obtaining laminar flow on two-dimensional wings.

* Published with the permission of the Director, National Physical Laboratory.

The present experiment was devised in order to extend the application of boundary-layer control to the establishment of laminar flow over fuselages and similar bodies. Away from the forward stagnation point, the essential differences between a two-dimensional aerofoil and a body are the surface curvature of the latter in planes transverse to the flow, and the markedly smaller pressure gradients. A fuselage may also be subject to regions of three-dimensional boundary-layer flow (as on a swept-back wing), if it is of an unsymmetrical form. It was decided, however, for ease of manufacture, to approximate to a fuselage shape in the first case by constructing a body of revolution, on which regions of three-dimensional flow could be obtained quite simply by setting the body at an angle of yaw to the flow. It was hoped to find out whether these departures from two-dimensional flow conditions had any fundamental effect on the use of boundary-layer suction for maintaining laminar flow.

In the practical application to an aircraft, it is evident that if a worthwhile drag reduction is to be obtained, it will be necessary to preserve laminar flow downstream of the junction of the wing and the fuselage. The body of revolution was therefore designed to include a wing root over which suction could be applied and special attention was given to this region. This design solved another problem: it enabled the body to be suspended in the wind tunnel from its wing, thus avoiding the use of either a sting mounting or of supporting wires or struts over the front portion of the model where the intersection of the supports with the body would have given rise to unwanted wedges of turbulent boundary layer.

Exploratory work was also carried out with isolated excrescences on the surface of the solid body. The critical heights of excrescence just causing wedges of turbulent flow were measured, and a comparison was made with similar measurements on a two-dimensional boundary layer.

2. *Design of the Body of Revolution.*—In order to be somewhat representative of the fuselage of a modern aircraft, the body was designed to have a fineness ratio of 10, and to be coupled with a wing of chord equal to $1\frac{1}{3}$ times the maximum diameter of body. It was also necessary at the start to select the method of applying suction, either through circumferential slits or porous strips, or else distributed over the surface. The latter arrangement was chosen in view of the possibility of severe demands in the vicinity of the wing-body junction, although it appeared to present a more difficult constructional problem, especially as suction was required all the way round the body, thus precluding access to the interior. Experience with laminar flow on two-dimensional aerofoils has suggested that the external pressure gradients are not of great importance when the boundary layer is kept under control by suction. It was therefore decided to avoid the construction of a porous surface with double curvature by confining distributed suction to the central third of the length of the body, which would simply be a cylinder. As such a shape implies the existence of adverse velocity gradients ahead of the cylindrical region, a preliminary experiment was planned with a quickly made solid version of the body (Section 3) to ascertain whether laminar flow would reach the cylindrical portion or whether some preliminary boundary-layer control would be necessary (Section 4).

The ordinates determining the external outline of the body are given in Appendix I, and the shape is shown in Fig. 1, which also marks the porous area. The 15-ft long body was constructed of three portions of equal length, the central cylindrical portion of the solid version being replaced later by the porous cylinder and porous wing combination. The shape of the rear portion was not considered to be very important. For the first foot of its length it remained cylindrical (diameter 18 in.) and was then faired into a straight conical tail with a surface whose generator was a portion of a circular arc.

The length/maximum radius of the nose portion of 6·7 was sufficiently large to ensure that the inevitable fall in velocity ahead of the cylindrical portion would not be sufficient to provoke laminar separation. For convenience, the shape adopted for the nose portion was the smooth curve of the forward half of one of the streamline bodies designed by Young and Owen[2] and experiment showed (Fig. 2) that the velocity distribution over this arbitrary combination was satisfactory. Although a more refined design would probably have reduced the adverse velocity gradient, the peak velocity was only 1·04 of the stream velocity.

The supporting wing for the porous version of the body was chosen to be 18 per cent thick and of 2-ft chord. The section was RAE 104.

3. *Details of the Solid Version of the Body and Instrumentation.*—The three portions of the non-porous version of the body were built up from pine planks glued to a number of hollow wooden rings. Accurately fitting joints were assured by using turned metal rings extending to the surface at these positions. The surface was hand-rubbed until it matched the curve of a master template whose waviness was ascertained to be less than $\pm$ 0·003 in. on a 3-in. gauge length. The surface was finished with black Phenoglaze Lacquer and polished, thus facilitating the use of the china-clay method of indicating transition. Pressure-plotting holes were provided along a horizontal and a vertical generator over the forward half of the model ; the leads were brought out of the model at the tail end.

The model was suspended in the N.P.L. 13-ft $\times$ 9-ft Wind Tunnel using a system of bracing wires attached at the mid-length position and close to the tail of the model. A comb of total-head tubes traversing the wake was mounted close behind the tail of the model. Assuming that the wake was axisymmetric in shape, this enabled an approximation to the drag of the body to be quickly found.

4. *Transition and Drag Measurements on the Solid Body at Zero Yaw.*—The model was first suspended in the wind tunnel at zero yaw, under which conditions the velocity distribution over the surface was as shown in Fig. 2. The variation of transition position with wind speed, as determined by the china-clay method, is given in Fig. 3. The data have been replotted in Fig. 4 in non-dimensional form, showing the variation of Reynolds number at transition ($U_1 s/\nu$) with the flow Reynolds number based on body length ($U_0 l/\nu$). The maximum value of the transition Reynolds number, $4\frac{1}{2}$ million, is low compared with the value obtained on two-dimensional aerofoils. This is presumably due to the smaller stabilizing effects of the less favourable velocity gradients over the front of the body, although a more sophisticated explanation on the basis of stability theory has recently been advanced by Smith and Gamberoni[3].

Also plotted in Fig. 4 are the results of recent tests on bodies carried out in America[4] and the corresponding velocity distributions are shown in Fig. 5. Several interesting features emerge from the comparison. Where bodies of the same general shape are tested in the same wind tunnel (the N.A.C.A. prolate spheroids) the greater maximum Reynolds number at transition is obtained on the fatter body (smaller fineness ratio), again presumably owing to the influence of the velocity gradients. It is surprising that where transition falls between 0·3 and 0·4 of the body length, the body tested in the N.P.L. 13-ft $\times$ 9-ft Wind Tunnel shows up so well compared with the N.A.C.A. bodies. The velocity distribution on the N.A.C.A. body of fineness ratio 7·5 is closely similar to that on the present body, whilst the turbulence level in the 13-ft $\times$ 9-ft Wind Tunnel is of the order of 0·16 per cent compared with less than 0·02 per cent in the Ames 12-ft Tunnel. The reduction in transition Reynolds number on the N.P.L. body when transition moves forward of about 0·3 of the length, despite the favourable gradient, is due to the increasing turbulence of the 13-ft $\times$ 9-ft Wind Tunnel at its top speed (similar forward movements of transition as this speed has been approached have been observed on two-dimensional aerofoils). It is suggested that the different shape of the curve for the N.P.L. body, when transition is aft of the 0·4-length position is due to the destabilising effect of the adverse velocity gradient which exists aft of 0·3 of the length. This was thought not to matter as the boundary layer would come under the control of the distributed suction in this region of the body.

However, Fig. 3 shows that transition moves forward of 0·33 chord above a wind speed of about 130 ft/sec so that it was necessary to apply some form of boundary-layer control over the nose of the model. This was done by inlaying a porous strip at 0·2 of the length and a small amount of suction was found to delay transition to the cylindrical portion of the body up to the top speeds of the tunnel.

Assuming axisymmetrical flow, the values of the drag coefficient (based on wetted area of surface) worked out from the wake traverse readings are plotted as a function of Reynolds

number in Fig. 6, and compared with the laminar and turbulent flat-plate skin-friction coefficients. The form drag of the body (fineness ratio 10) is seen to be small, and owing to the low transition Reynolds number, the scope for drag reduction by laminarization is apparent. Also shown on the Figure are the drag coefficients measured in the 13-ft × 9-ft Wind Tunnel on the Handley-Page laminar-flow wing, indicating the drag reduction obtained when transition moved from 0·28 chord (porous strip surface) or 0·41 chord (plain surface), without suction, to 0·93 chord with suction.

5. *Effect of Yaw on Transition.*—Records of the transition front were also obtained over a wide range of wind speed with the body set at angles of yaw to the wind. A plan view of the body is shown in Fig. 7a, which gives the notation distinguishing the various generators, and Figs 7b and 7c show developments of the surface of the body with the transition fronts marked in for angles of yaw of 0 deg, 2 deg, 3 deg and 5 deg. The associated velocity distributions along the four principal generators with the body at 5 deg of yaw are given in Fig. 8.

The results show that the flow is quite different from the two-dimensional flow about an aerofoil. Although at 5-deg incidence the velocity along the generator which lies in the direction of increasing incidence (starboard side, Fig. 7a) is greater than that along the diametrically opposite generator, the changes are very small compared with those on a two-dimensional aerofoil and the velocity gradients remain favourable over the first 0·3 of its length. The transition position along these generators, however, is scarcely affected. Instead, transition moves markedly forwards along the two generators at right angles (top and bottom, Fig. 7a). This is due not to the streamwise velocity gradients, but to the transverse gradients. The flow is a curved one ; the streamlines diverge from the port side of the body (Fig. 7a) and, passing over both top and bottom generators, converge on the starboard side. The forward movement of transition is due to the instability of the resulting three-dimensional boundary layer, a phenomenon which was later discussed by Gregory, Stuart and Walker[5].

It should be noted that even at 2-deg angle of yaw, transition is affected at a wind speed of 120 ft/sec or greater. As a pilot flying without special instruments is liable to yaw an aircraft to this extent, the effect of suction on the phenomenon is of great practical importance if a laminar-flow body is to be achieved. This part of the experiment is discussed in Section 11.

6. *Precipitation of Transition by Isolated Excrescences.*—The opportunity was taken of screwing adjustable 60-deg conical excrescences into the surface at a number of positions and measuring the critical excrescence heights which first precipitated wedges of turbulent flow, as detected by the china-clay technique. This experiment was confined to zero angle of yaw and thus repeated for an axisymmetrical boundary layer the earlier work of Gregory and Walker[6] carried out in two-dimensional flow.

The critical excrescence height is plotted as a function of position and wind speed in Fig. 9. As was found in the case of the two-dimensional experiments carried out on a flat plate and on an aerofoil with zero pressure gradient, there was a considerable range of excrescence heights over which the observed phenomena altered. The lowest plotted value of the critical height is that at which a vague turbulent wake first appeared (*i.e.*, probably intermittent in character) spreading from a point well downstream of the excrescence. The largest values plotted refer to the excrescence height which produces a firm wake although this may start several inches downstream of the excrescence itself, a further increase in excrescence height being required to bring the apex of the wedge of turbulent flow to the excrescence itself. The earlier experiments showed that such a range of critical excrescence heights only exists with negligible pressure gradients and it is most marked only at low speeds. At a wind speed of 60 ft/sec, 5 ft from the nose of the body, for example, a faint wedge of turbulent flow was first noticed with an 0·037-in. excrescence, but a height of 0·049 in. was required to shift the apex of turbulent flow to the excrescence itself. At 180 ft/sec, 3 ft from the nose, an increase in excrescence height from 0·012 in. to 0·013 in. encompassed the change.

The analysis of the observations and a comparison with the results obtained from the tests carried out on a two-dimensional aerofoil, without going to the elaboration of the earlier empirical analysis, is a matter of some difficulty. This is because although various very simple criteria have been proposed to determine the critical heights of excrescence, the data obtained in the N.P.L. 13-ft. × 9-ft Wind Tunnel for both the two-dimensional and axisymmetrical boundary layers do not follow these rules closely throughout the wind-speed range of the tests. This was in fact the reason for the complication of the original analysis.

The development of the boundary layer on the body was calculated approximately by the methods of Wieghardt[7] and Thwaites[8] and checked satisfactorily with experimental boundary-layer traverses except in the region downstream of the velocity peak at 0·3 of the length. The traverses were not taken along the same generator of the body as the static-pressure observations, and the discrepancy is probably due to a variation of the local pressure distribution round the body. The boundary layer, and especially the skin-friction coefficient, would be expected to be sensitive to such variations in a region of local adverse gradient.

The comparison has been made between the critical excrescence heights obtained on the body and the results obtained by Gregory and Walker[6] on A.D.8 aerofoil at + 2-deg incidence. This was the incidence at which there was negligible favourable pressure gradient and the pressure distribution was closest to that over the body. An unpublished analysis by Klanfer and Owen (of the Royal Aircraft Establishment) of results obtained in two-dimensional flow conditions suggested that above a boundary-layer Reynolds number based on displacement thickness, $R_\delta{}^*$, of 1000, wedges of turbulent flow were caused if the Reynolds number $\varepsilon U_\tau/\nu$ exceeded 20. Fig. 10, which shows a plot of the results on this basis for both the body† and the aerofoil, suggests that the critical value of $\varepsilon U_\tau/\nu$ for the body is slightly higher than for the aerofoil and may be taken as about 23. It can be seen clearly from Fig. 10, as already pointed out, that the observations at any given excrescence position do not yield a constant value of $\varepsilon U_\tau/\nu$, but one which decreases steadily with increase of wind speed, typical curves being marked on the Figure.

If the comparison is made for values of $\varepsilon U_\varepsilon/\nu$, or even for $\varepsilon U_1/\nu$, as is suggested by von Doenhoff and Horton[9], it is again found that the critical values of these parameters for the flow over the body of revolution are up to 10 per cent higher than for the flow over two-dimensional aerofoil. These small differences are probably of no significance and it is concluded that for practical purposes the sensitivity of an axisymmetrical laminar boundary layer to the disturbances associated with isolated excrescences is the same as for two-dimensional flow.

7. *Details of the Porous Body and Instrumentation.*—The porous body of revolution is illustrated by photographs in Figs. 11 and 12 whilst its method of construction is revealed by the cut-away drawing (Fig. 13).

A fresh wooden nose was constructed for this model. It was made in two pieces, sandwiching a porous ring at $0{\cdot}2l$ from the nose. The flush fitting surface of the ring was Perflec electro-deposited mesh 0·036 in. thick with 80 × 80 apertures/sq. in., each aperture being 0·0055 in. square. The mesh was backed by a $\frac{1}{2}$ in. wide layer of Monel-metal wire cloth, 320 × 20 weave, which had been rolled until its thickness had been reduced from about 0·022 in. to 0·015 in. and which provided sufficient resistance to ensure uniformly distributed suction into the porous strip.

The porous central third of the body was constructed integral with the porous wing from which it was carried in the tunnel, and through which the suction piping carried the sucked air out of the tunnel. The main structural tubes carry the ribs and frame rings which support the basic 16 S.W.G. aluminium skin, coarsely perforated with 30 $\frac{1}{8}$-in. diameter holes/sq in. The external skin panels were cut from 26 S.W.G. aluminium sheet perforated with 576 0·0235-in.

† The observations of critical excrescence height taken on the body downstream of the $0{\cdot}33l$ station have not been plotted in Fig. 10a. This is because these positions are in the region where the boundary layer was not as calculated, and the estimation of U_τ would have been subject to some error.

diameter holes/sq in. The longitudinal edges of the panels on the body were cut at an angle of 15 deg to the line of the generators (Fig. 14) so as to lie at an angle to the flow, and were reinforced with 0·030-in. × $\frac{1}{4}$-in. strips. The panels were screwed to the basic perforated surface sandwiching between them a layer of porous material of sufficient resistance to ensure a uniform distribution of suction. It was intended to use a number of layers of filter paper as resistance thus enabling some control of the suction distribution to be exercised, even to the extent of blanking off portions of the skin with an impervious layer of paper, as had been done on a previous experiment with a porous nose[10]. Unfortunately it proved impossible to tension the external skin, so that when suction was applied, the filter paper bedded down and left a gap under the outer skin. This permitted circulation of the air through the perforations of the outer skin and extraneous wedges of turbulent boundary-layer flow occurred which could not be prevented by adjustment of the suction rate. This difficulty was overcome by replacing the filter paper by a single layer of Porvic microporous plastic filter sheeting 0·03 in. thick which was stuck* on to the under surface of the outer panels. This material had a high resistance to flow (passing 1 cu ft/sec/sq ft for a pressure of 10 in. water gauge), and it was found to clog with dust less rapidly than filter paper. It was not possible with Porvic to alter the resistance of the porous skin locally or to block areas up.

Some control of the suction was obtained, however, as the body was divided into four suction compartments each with a separate suction tube, flow meter and control valve. The arrangement of the suction compartments is shown in Figs. 13 and 14, the porous strip, the wing-root junction, the rest of the wing and the remainder of the body being separately controlled.

The model was suspended from the roof-balance in the 13-ft × 9-ft Wind Tunnel, so that its drag could be measured. The connection to the balance was a pin-joint, AA in Fig. 15, and sway of the model was prevented by transverse bracing attached to wing and tail and carried in streamline fairings (Fig. 12). The wires were adjusted to be accurately normal to the fore and aft movement of the drag frame to avoid constraint on the drag measurement. The metering pipes were carried above the wing, and the connection to suction pipes fixed to earth was made *via* an ' air bearing ' in order to avoid constraint. The design of the air-lubricated flanges is shown in Fig. 16 and they proved completely satisfactory in use.

The model was carefully rigged to zero incidence by adjustment of the length of one of the support tubes. Provision for yaw up to 5-deg incidence was made by movement of the member carrying the pin-joints AA relative to the rest of the drag frame.

The state of the flow in the boundary layer was determined in a number of ways. For obtaining an overall picture under given conditions, surface indicator techniques were used : the china clay method was used on the solid portions of the model, whilst on the perforated skin the sublimation of naphthalene provided a faint indication of the transition front. The naphthalene was dissolved in acetone and applied as a dry spray (*i.e.*, the acetone evaporated before the naphthalene reached the surface) and it was found that clogging of the pores did not occur. For investigating the effect of suction on the flow at discrete points on the model, total-head tubes were affixed to the surface and connected to a microphone and amplifier and used as acoustic detectors of turbulence.

Boundary-layer traverses were undertaken with a remotely controlled traversing probe and yaw-meter[11]. For traverses in the vicinity of the wing-root junction, the mechanism was carried on an arm attached to the wing itself ; for traverses towards the rear of the body, the mechanism was mounted on a tripod on the floor of the tunnel. The wake comb was also used in the position illustrated in Fig. 12, but the drag evaluated was only meaningful when the body was at zero incidence and yaw.

* Dilute Titebond adhesive was sprayed on to the undersurface of the external perforated panels and allowed to dry ; this could be done without blocking the perforations. The Porvic sheeting was sprayed with acetone and brought into contact with the prepared surface and allowed to dry without further movement. As the adhesive was soluble in acetone, a bond was formed, but care had to be taken as the Porvic also was softened but no permanent adverse effects were discovered after the acetone had evaporated.

8. *The Extension of Laminar Flow with Distributed Suction.—Transition, Drag and Boundary-Layer Measurements at Zero Yaw.*—Considerable difficulty was experienced in extending laminar flow over the porous surfaces of the wing and the body with suction, and it became obvious that the external porous surface was not good enough for the purpose. It has already been mentioned that the impossibility of tensioning the perforated skin when fitting it to the body necessitated sticking the porous backing underneath the perforated skin. The same lack of fit showed up in imperfectly matched circumferential joints between successive sheets wrapped round the body. The wedges of turbulent flow which originated at the joints were eliminated at the lower tunnel speeds by fairing the slight steps between adjacent sheets with Plasticene, but this procedure was not satisfactory at the higher wind speeds.

The experimental technique adopted for obtaining laminar flow was to mount a number of acoustic probes on the porous surface and to observe the suction flow rates at which the turbulent boundary layer became intermittent, laminar and finally completely stable. When no improvement was possible, or if the flow became turbulent again with increasing suction, the sublimation technique was used, which generally showed that an imperfection in a skin joint required improvement. By this means (once the filter paper had been replaced by Porvic), it was found possible to obtain laminar flow at least as far back as the rear edge of the perforated sheet on the wing (0·90 chord) with a minimum mean suction velocity ratio whose value decreased steadily from 0·0033 at a wind speed of 60 ft/sec to 0·0022 at 180 ft/sec. These suction ratios are just a little extravagant, but in the absence of any form of control of the porous resistance it was impossible to reduce the suction over the forward part of the aerofoil where it was unnecessarily large. The only skin joints which the laminar flow had to surmount were those at the ends of the perforated skin at 0·1 and 0·9 chord. These, however, were joints where the metal skin was screwed to the wood and gave no trouble. Some boundary-layer traverses were later carried out on the wing and are described in Section 10.

On the body, attention was first concentrated on regions away from the wing-root junction and after careful fairing of all skin joints and the elimination of roughness, laminar flow was obtained on the undersurface back onto the wooden tail cone at a wind speed of 80 ft/sec. Transition was at $0{\cdot}82l$ compared with $0{\cdot}41l$ without suction at the same speed. The minimum suction velocity ratio required to achieve this result was $v_0/U_0 = 0{\cdot}00064$ on the porous cylinder with additional suction on the porous strip round the nose. It was not possible to oversuck (within the limitations of the pumping equipment), laminar flow still being obtained at the maximum available rate of 0·0029.

At a wind speed of 100 ft/sec, disturbance-free laminar flow reached the porous cylindrical surface over most of the circumference only after careful attention had been given to the joints between the porous ring and the rest of the nose. In this respect the porous ring on the original nose had been more satisfactory. However, it proved impossible at this wind speed to keep the flow laminar behind either the first or second porous skin joints, whilst in the region of the wing-root junction transition occurred ahead of the wing.

The best transition front recorded at this stage of the investigation at a wind speed of 80 ft/sec is drawn on a development of the surface of the model in Fig. 17 and can be compared with the zero suction record of Fig. 18. The transition record with suction is also shown in the photograph of the model (Fig. 12). Boundary-layer profiles were measured at the positions marked A and B in Fig. 17 and the profiles taken at the latter position are shown in Fig. 19. The variation of boundary-layer Reynolds number (R_δ^*) with the suction velocity ratio is shown in Fig. 20. The cylindrical porous portion is long enough for asymptotic conditions to be reached, but the maximum value of R_δ^* reached with the minimum suction to keep the flow laminar, is only 1360. In comparison at the same wind speed and in the same tunnel, the tests on the two-dimensional laminar-flow wing[1] gave values of R_δ^* between 1800 and 2400 just upstream of the porous strips, so that the unsatisfactory nature of the perforated surface and skin joints is apparent.

The drag of the complete model was measured on the overhead balance and the wake drag of a section underneath the body was obtained from a wake traverse comb at the tail. The readings and their analysis are set out in detail in Appendix II. Comparison of the wake traverse drag measurements without suction suggests that the drag of the porous body is 12 per cent greater than that of the smooth solid body, when transition wires were fitted at the nose, and 34 per cent greater when natural transition occurred. The position of natural transition was only slightly different in the two models as it was close to the start of the porous section, but the measurements do suggest that the porous surface was not aerodynamically smooth.

The measured velocity distribution (Fig. 2) shows that the static pressure over the porous section of the model is only very slightly below the free-stream value. With suction, therefore, neglecting the resistance of the porous surface to the suction inflow and assuming equal propulsive and pumping efficiencies, the ideal effective drag coefficient is the sum of the wake drag coefficient and the suction quantity coefficients. The wake traverse measurements thus show that with suction, the ideal effective drag of a porous body without wing would be 45 per cent of the drag of the same body with natural transition and would be 60 per cent of the drag of the smooth solid body. These high percentages would be much reduced at higher Reynolds numbers if laminar flow could be obtained, as the extent of laminar flow occurring naturally would be much less. They would be still further reduced and the drag closer to the flat-plate value if the porous body had been designed for laminar flow over its full length. With the present body, it is very satisfactory to obtain laminar flow over 82 per cent of its length whilst the surface is only porous back to 67 per cent of its length.

The balance measurements of the drag of the complete model also show that the gains due to suction are small, but the analysis of the measurements suggests that this is because the increase in the area of laminar flow obtained by suction (*see* Figs. 17 and 18) is not large. The area of turbulent boundary layer on the body arising from the vicinity of the wing root nearly doubles the drag of the body over what it would have been had the best transition position been maintained all the way round the circumference. Similarly, the increased extent in laminar flow on the wing is only obtained over half the span. The difference between the wake drag (balance drag minus sink drag) of the wing-body combination and the sum of the values estimated for the two components has been designated the interference drag. This also is decreased slightly by suction. This is only true if the drag arising from the turbulent wakes on the body is regarded as part of the body drag : if this proviso is neglected, the interference drag rises with suction (it should be pointed out that there was no turbulent-flow wedge without suction as transition was then ahead of the leading edge of the wing).

Attempts were made to eliminate the turbulent boundary-layer wedge on the body (Fig. 17), but without complete success. The wedge arose partly from the box-body skin panel joints and partly from the secondary flow at the wing-body intersection. Boundary-layer traverses and tuft studies carried out in the area in front of the wing and described in Section 9, revealed that distributed suction reduced the secondary flow in the boundary layer. But the flow direction was largely along the inclined line which marked both the division of the wing-root suction box from the rest of the body and also an external skin joint ; this coincidence was responsible for a wedge of turbulent flow. It was eliminated by altering the shape of the external skin panel (Fig. 21), but further wedges associated with skin joints and the box division appeared. Further improvements were not attempted since attention to the turbulent-flow wedge at the wing-body intersection revealed a serious fundamental difficulty. Although various solid fillets and fairings were ineffective, the turbulent wedge was successfully eliminated when all fillets were removed and the two porous surfaces, wing and body, were allowed to intersect at right angles. The flow in the corner then remained laminar right back to the trailing edge of the wing. Here, however, a new wedge of turbulent boundary layer appeared (Fig. 21). The investigation described in Section 10 suggested that this wedge was due to the contamination of the boundary layer on the body by the extremely rapid development of turbulence in the wake from the wing and the successful treatment of this problem would have required extensive modifications to the model that were not practical with the present method of construction.

9. *The Boundary Layer at the Front of the Wing-Root Junction.*—The velocity distribution over the front of the body in the vicinity of the wing root was determined by traversing a static tube over the surface. The isobar pattern is shown in Fig. 22 whilst Fig. 23 shows, to a larger scale, the positions chosen for boundary-layer traverses.

At position A (Fig. 23) the boundary-layer flow was unidirectional, but at position B, appreciable secondary flow was present and the components of the measured profiles are shown in Fig. 24. Without suction, the flow was turbulent, there was 11 deg of twist in the direction of the velocity vector across the thickness of the boundary layer and the value of χ, the cross-flow boundary-layer parameter, was 1900. With suction, the angle of twist increased to about 20 deg, but the boundary layer was thinned so that χ was reduced to 1180 and the flow was just laminar. This is a remarkably high value of χ at which to obtain laminar flow and the result must be regarded with some suspicion. No great accuracy is claimed for the yaw-meter traverses, but the result may in part be due to the closeness to the surface of the position of the velocity maximum, which exercises a stabilising effect on the stability of the cross-flow profile. The secondary flow at positions C and D was less severe than at B, so that no difficulty was experienced in obtaining laminar flow with suction.

The rate of suction applied locally over the area of the wing-root suction box to maintain laminar flow in the intersection was a v_0/U_0 of 0·00317 compared with the value, v_0/U_0 of 0·00088, used over the rest of the body. The effect of a much greater local suction rate, v_0/U_0 of 0·0185 was to generate a turbulent boundary layer at position B. This was thought to be due to roughness effects of the joint between the box and the surrounding skin panels.

10. *The Boundary Layer at the Rear of the Wing-Root Junction.*—The most favourable transition front on the body in the vicinity of the wing-root junction (with suction applied) at a wind speed of 80 ft/sec has been illustrated in Fig. 21. Apart from the wedges of turbulent flow whose cause is either breaks in the continuity of suction or roughness at skin joints, a wedge of turbulent boundary layer was observed originating from the intersection with the body of the trailing edge of the wing, and this wedge could not be eliminated by adjustment of the suction rate.

Velocity traverses were therefore made in the flow over the rear part of the wing, and the velocity profiles at stations 0·90, 0·995 and 1·02 chord are shown in Fig. 25 for the case with the normal suction velocity ratio for the wing, a v_0/U_0 of 0·00257. Owing to the absence of distributed suction over the last 10 per cent of the chord it was found that the boundary layer thickened appreciably, and owing to the adverse velocity gradient the profile tended towards a separation-type profile. However, the stethoscope showed that immediately the boundary layer left the trailing edge and became a wake, bursts of turbulence started and only 0·5 in. downstream from the trailing edge, the flow was completely turbulent.

It thus appears that despite distributed suction, a wedge of turbulent boundary layer on the body is precipitated by the turbulent flow in the wake of the wing outside the body boundary layer. Even with the very high suction velocity v_0/U_0 of 0·015, the value of R_δ* for the boundary layer on the wing increases from about 210 at 0·9 chord to 1100 at 0·995 chord, and is correspondingly larger with less suction. Also, it may be inferred from the experiments of Hollingdale[12] that the critical R_δ* for stability of a laminar wake is only of the order of 50. Hence it would appear that only almost complete withdrawal of the boundary layer into a slot at the trailing edge of the wing, or distributed suction right to the trailing edge, is likely to prevent the wake becoming turbulent and contaminating the laminar flow on the body downstream of the wing. As this would require extensive alterations to the model, and is more conveniently attempted on a part-model constructed specially for the purpose, the problem was not pursued further on the present model.

11. *The Boundary Layer due to Yaw.*—The transition pattern which was obtained when the body was set at 5-deg angle of yaw and the normal suction quantity was applied is shown in Fig. 26, which can be compared with Fig. 17 showing the pattern obtained at zero yaw.

The observations on the solid body (Fig. 7), had shown that the effects of the secondary flow were worst along the top and bottom generators of the body and that even at as low a wind speed as 80 ft/sec, the transition position along these generators was close to the start of the cylindrical section. Boundary-layer traverses were therefore undertaken at the various positions along the body indicated by A, B, C and D in Fig. 26 with the same minimum suction quantity required to maintain laminar flow in the absence of yaw, and also without suction.

The traverses showed, roughly, that at all the positions, A, B, C and D, the flow direction made an angle between 11 deg and 14 deg to the generator and that this angle was unaffected by the application of suction. The twist in the direction of the velocity vector through the thickness of the boundary layer was also small and could not be measured with any precision. At positions A and B the yaw-meter suggested angular changes of less than 1 deg, but the variation with height was irregular and cross-flow profiles could not be calculated. At the succeeding positions C, D, a regular twist of about 1·7 deg and 1·8 deg was observed without suction, and this decreased to 0·6 deg and 0·4 deg when suction was applied. From smooth curves drawn through the observations, the components of the velocity profile parallel and perpendicular to the external stream were calculated and these are given in Fig. 27. It will be seen that the suction quantity required to stabilize laminar flow has practically eliminated the secondary flow. This suggests that at this position on the body the continuance of laminar flow depends on the stability of the streamwise component of the boundary layer rather than on the crossflow components.

12. *Conclusions.*—Experiments were carried out in order to examine the application of boundary-layer suction to extend laminar flow and reduce the drag of a 15-ft long body of revolution of fineness ratio 10 : 1.

Tests on a solid version of the body showed that its drag was almost entirely skin-friction drag. Because of the very small favourable pressure gradients, the Reynolds number at transition based on the length of laminar flow reached a maximum of only $4\frac{1}{2}$ million at a body Reynolds number of 15 million, so there was ample scope for extending laminar flow. At angles of yaw it was found that the transition position was much closer to the nose along certain generators owing to the instability of the three-dimensional boundary layer.

The heights of isolated excrescences on the solid body just giving rise to wedges of turbulent boundary layer were measured and found not to differ appreciably from the heights of roughness which were critical on a two-dimensional aerofoil.

The suction version of the body was porous over the middle third of its length, which was cylindrical in form. A porous strip was fitted on the nose and the body was suspended from the tunnel balance by means of a stub wing which also was porous.

At 80 ft/sec wind speed, distributed suction (v_0/U_0 of 0·00088) extending back to 0·67 of the length enabled laminar flow to be maintained to 0·82 of the length on the parts of the body away from the wing-body intersection. At higher speeds, the joints in the perforated skin on the body proved to be too rough to allow laminar flow since numerous wedges of turbulent flow appeared, originating from the joints.

Distributed suction at the wing-body intersection reduced the secondary flow and enabled laminar flow to be obtained in this region, although difficulties were again encountered owing to awkward skin joints. But even with laminar flow around the intersection, a wedge of turbulent boundary layer on the body started downstream of the trailing edge of the wing owing to contamination from the laminar wake of the wing, which became turbulent downstream of the trailing edge. As complete withdrawal of the wing boundary layer either by extending distributed suction right to the trailing edge, or by installing a slot there, would have required considerable modification to the model, the problem of obtaining laminar flow on the body behind the wing was not followed up. It is suggested that the problem could best be tackled on a simple part-model made specifically for the purpose.

There was only a small reduction in the ideal effective drag of the complete model when the extent of laminar flow was increased by distributed suction. This was due partly to the large suction quantities required and partly to the considerable areas of turbulent flow which remained on both the wing and the body. However, the analysis of the drag observations suggests that much greater drag reductions could be obtained : (i) at higher Reynolds number (if the porous surface were sufficiently smooth), (ii) if the porous region were more extensive so that full-length laminar flow were achieved, and (iii) if the problem of contamination downstream of the wing were solved so that laminar flow could be obtained round the whole circumference.

The adverse effects of 5-deg yaw noticed on the solid body were not encountered with suction ; the suction quantity needed at 0-deg yaw to give far-back transition was also adequate at 5-deg yaw.

Acknowledgements.—The solid wooden version of the model was made by Mr. R. Coad and the porous version was designed by Mr. P. T. Taylor and constructed by Mr. W. L. Rich in the N.P.L. Aerodynamics Division Workshop.

LIST OF SYMBOLS

v_0	Suction velocity
u	Velocity in the boundary layer
U_0	Free-stream velocity
U_1	Velocity outside boundary layer
U_ε	Velocity at height ε from the surface (in absence of excrescence)
U_τ	Friction velocity $= \sqrt{(\tau_0/\rho)}$
x	Distance along chord
s	Distance round surface
c	Chord of aerofoil
l	Length of body
ε	Height of excrescence
δ	Thickness of boundary layer
δ^*	Displacement thickness of boundary layer
τ_0	Skin friction
ρ	Density
ν	Kinematic viscosity
R_l	Reynolds number based on length of body $= U_0 l/\nu$
R_s	Reynolds number based on distance round surface $= U_1 s/\nu$
R_δ^*	Boundary-layer Reynolds number $= U_1 \delta^*/\nu$
χ	Cross-flow boundary-layer parameter $= (u \sin \theta)_{\max} \delta/\nu$
C_F	Wake drag coefficient based on wetted area of body or wing ($C_F = F/\frac{1}{2}\rho U_0^2 A$)
C_Q	Suction-quantity coefficient based on wetted area of body or wing ($C_Q = Q/U_0 A$)
H	Boundary-layer shape parameter
α	Angle of yaw
θ	Angle of twist of boundary-layer velocity vector relative to the direction of flow outside the layer

REFERENCES

No.	Author	Title, etc.
1	G. V. Lachmann (Handley Page, Ltd.), N. Gregory and W. S. Walker (N.P.L.)	Handley-Page laminar-flow wing with porous strips : details of model and wind tunnel tests at N.P.L. A.R.C. 14,794. May, 1952.
2	A. D. Young and P. R. Owen ..	A simplified theory for streamline bodies of revolution and its application to the development of high-speed low-drag shapes. R. & M. 2071. July, 1943.
3	A. M. O. Smith and N. Gamberoni	Transition, pressure gradient and stability theory. Douglas Aircraft, Co. Inc. Report ES26388. August, 1956. A.R.C. 19,322. May, 1957.
4	F. W. Boltz, G. C. Kenyon and C. Q. Allen	Measurements of boundary-layer transition at low speed on two bodies of revolution in a low-turbulence wind tunnel. N.A.C.A. R.M. A56G17. NACA/TIL 5120. September, 1956.
5	N. Gregory, J. T. Stuart and W. S. Walker	On the stability of three-dimensional boundary layers with application to the flow due to a rotating disk. *Phil. Trans. Roy. Soc.* (A). 943. Vol. 248. p. 155. July, 1955. Also : Proc. N.P.L. Symposium.—Boundary layer effects in aerodynamics. 1955.
6	N. Gregory and W. S. Walker ..	The effect on transition of isolated surface excrescences in the boundary layer (Part I). R. & M. 2779. October, 1950.
7	K. E. G. Wieghardt	On a simple method for calculating laminar boundary layers. *Aero. Quart.* 5. p. 25. 1954.
8	B. Thwaites	Approximate calculation of the laminar boundary layer. *Aero. Quart.* 1. p. 245. 1949.
9	A. E. von Doenhoff and E. A. Horton	A low-speed experimental investigation of the effect of a sandpaper type of roughness on boundary-layer transition. N.A.C.A. T.N. 3858. October, 1956.
10	N. Gregory and W. S. Walker ..	Wind-tunnel tests on the NACA 63A009 aerofoil with distributed suction over the nose. R. & M. 2900. September, 1952.
11	D. W. Bryer	A remotely-controlled traversing yaw-meter for boundary-layer exploration. *J. Sci. Inst.* 33. p. 173. 1956.
12	S. H. Hollingdale	On the stability and configuration of the wake produced by solid bodies moving through fluids. *Phil. Mag.* (7) 29. p. 209. 1940.

APPENDIX I

Shape of Body of Revolution and Supporting Wing

Body of Revolution . . . . . Length overall 15 ft

Fineness ratio 10

Nose portion

$0 \leqslant x \leqslant 60$ in. . . . . Radius of curvature of generator at nose 0·666 in.

x (in.)	Radius (in.)	x (in.)	Radius (in.)
0	0	30	7·003
3	2·102	36	7·616
6	3·065	42	8·143
12	4·444	48	8·568
19	5·477	54	8·861
24	6·302	60	9·000

Centre portion

$60 \leqslant x \leqslant 120$ in. . . . . Radius is 9·00 in. constant

Tail portion

$120 \leqslant x \leqslant 132$ in. . . . . Radius is 9·00 in. constant

$130 \leqslant x \leqslant 146{\cdot}6$ in. . . . . Generator is a circular arc of radius 68·152 in.

$146{\cdot}6 \leqslant x \leqslant 180$ . . . . . Surface is conical with a semi-angle at the tail of $12\frac{1}{2}$ deg.

Supporting Wing . . . . . Chord . . . . . 2 ft

Thickness/chord ratio 0·18

Section . . . . RAE 104

APPENDIX II

Measurements and Analysis of Drag of Body of Revolution

Notation: C_F = Wake drag coefficient based on wetted area of body or wing (as appropriate)

(*a*) *From Wake Traverse Measurements in Line with Bottom Generator on Solid Body*

Wind speed (U_0 ft/sec)	Reynolds number	Transition position (x/l)	Measured C_F from single wake traverse	Equivalent drag of body (lb)	Calculated drag at 80 ft/sec (lb)
60	$5{\cdot}76 \times 10^6$	0·47 (Natural transition)	0·00226	0·54	0·96
120	$1{\cdot}15 \times 10^7$	0·36 (Natural transition)	0·00236	2·26	1·00
180	$1{\cdot}73 \times 10^7$	0·23 (Natural transition)	0·00246	5·29	1·04
120	$1{\cdot}15 \times 10^7$	0·017 (Wire)	0·00314	3·01	1·42

(*b*) *From Wake Traverse Measurements in Line with Bottom Generator on Porous Body*

Wind speed (U_0 ft/sec)	Reynolds number	Transition position (x/l)	Effective C_Q based on gross body area	Measured C_F from single wake traverse	Equivalent drags for porous body without wing	
					Sink drag (lb)	Wake drag (lb)
		0·017 (Wire)		0·00373		1·59
80	$7{\cdot}7 \times 10^6$	0·37		0·00314		1·34
		0·82	0·00043	0·00097	0·36	0·42

(*c*) *From Wake Traverse Measurement behind Trailing Edge of Wing*

Wind speed (U_0 ft/sec)	Reynolds number	Transition position (x/l)	C_Q†	Measured C_F†	Calculated C_F† for smooth wing
		0·05			0·0073
80	$1{\cdot}02 \times 10^6$	0·50			0·0049
		1·0	0·00206	0·00146	

† Coefficients evaluated on wetted area of wing.

(*d*) *From Balance Measurements on Body and Wing*

Wind speed U_0 : 80 ft/sec

Body Reynolds number $U_0 l/\nu$: $7{\cdot}7 \times 10^6$

Wing Reynolds number $U_0 c/\nu$: $1{\cdot}02 \times 10^6$

Transition position on body (x/l)	Transition position on wing (x'/c)	Overall balance drag (lb)	Overall sink drag (lb)	Overall wake drag (lb)	Estimated breakdown of wake drag		
					Body drag (lb)	Wing drag (lb)	Interference drag[5] (lb)
0·017 (wires)	0·05	2·52	0	2·52	1·59[1]	0·47[3]	0·46
0·37	0·65 solid 0·45 porous	2·06	0	2·06	1·34[1]	0·35[3]	0·40
0·82 (best)	0·65 solid T.E. porous	1·79	0·53	1·26	0·76[2]	0·19[4]	0·31

(1) From wake traverse measurement

(2) From wake traverse measurement, but increased from the value 0·42 to allow for the areas of turbulent flow

(3) Calculated (Squire and Winterbottom) using observed transition points and making allowance for roughness of porous surface as deduced from wake traverse measurements on the solid and porous bodies

(4) From boundary-layer traverse at trailing edge on porous portion, and calculated for solid portion

(5) By subtraction.

(*e*) *Distribution of Suction*

	Porous strip	Porous body	Wing-root suction box	Wing
Percentage of total flow	9	56	18	17
Velocity ratio into surface v_0/U_0	0·025	0·00088	0·00317*	0·00257
C_Q based on gross body area	0·000056	0·000346		
C_Q based on wing wetted area				0·00206

* *Note.*—The suction flow into the wing-root box is at a rate 3·6 times as fast as into the rest of the body, or 1·22 times as fast as into the rest of the wing.

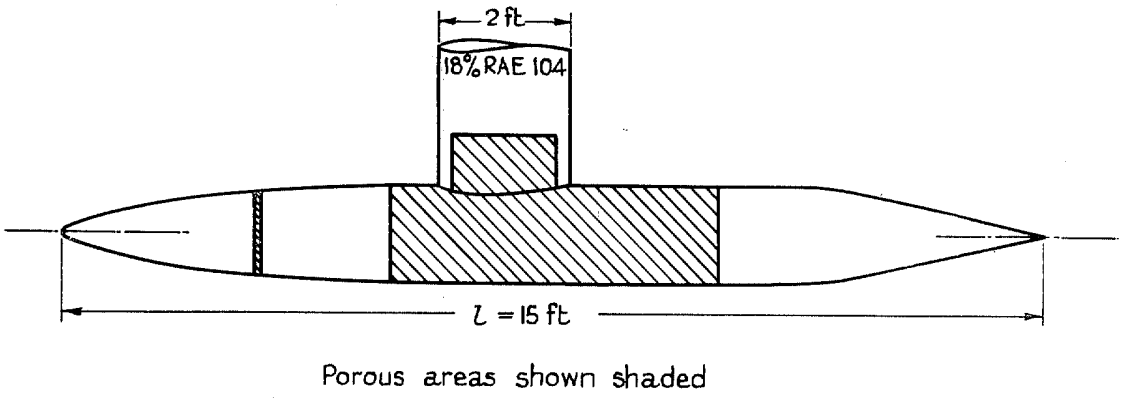

FIG. 1. Elevation of body of revolution.

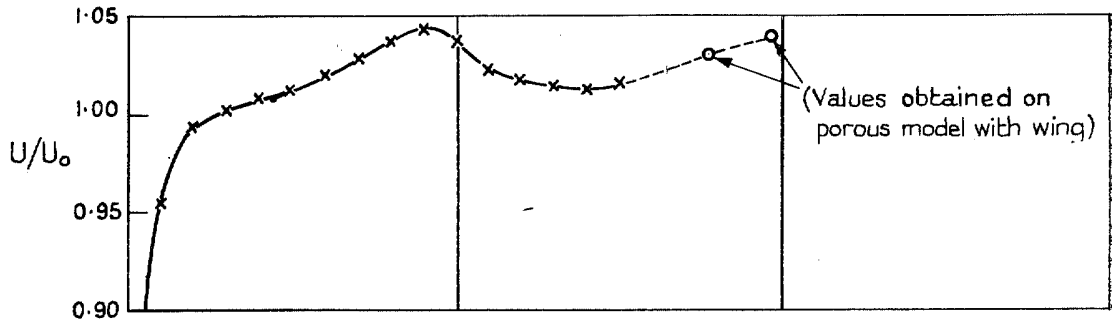

FIG. 2. Measured velocity distribution on solid model (without wing).—Zero yaw.

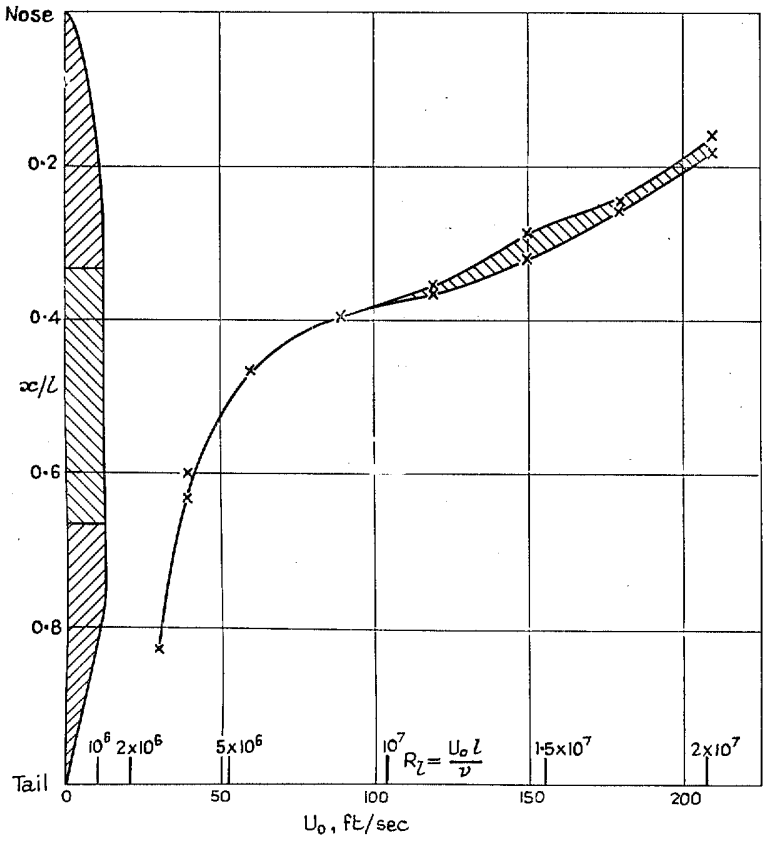

FIG. 3. Variation of transition position with wind speed or length Reynolds number on solid body.

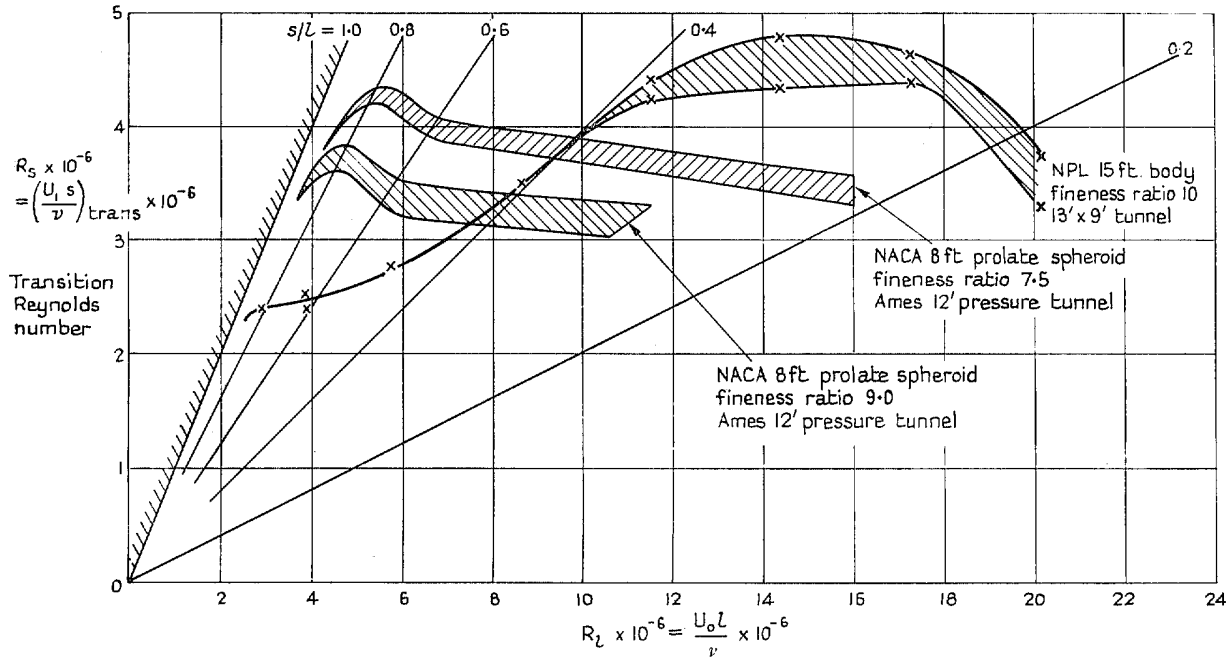

FIG. 4. Variation of transition Reynolds number with length Reynolds number for various bodies.

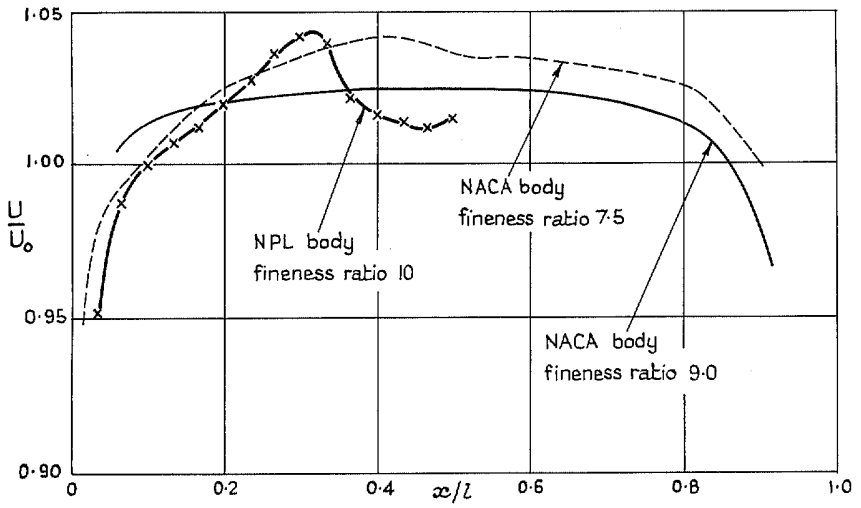

FIG. 5. Velocity distributions on various bodies.

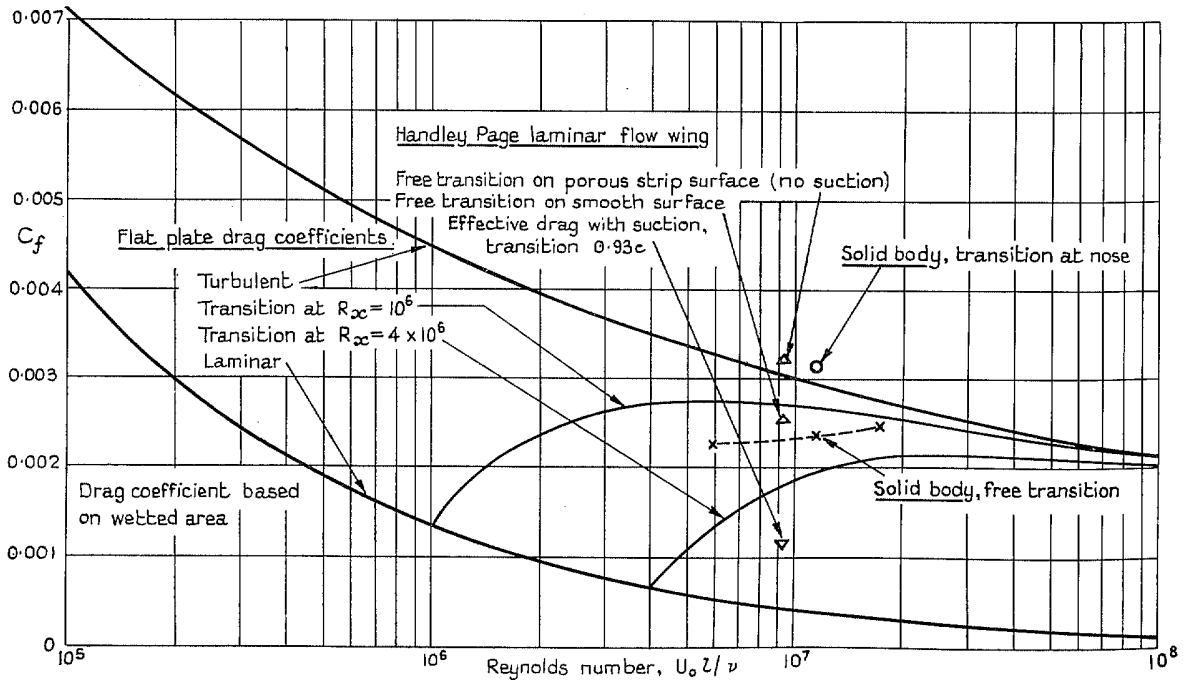

FIG. 6. Relation between drag coefficients of body and of a flat plate.

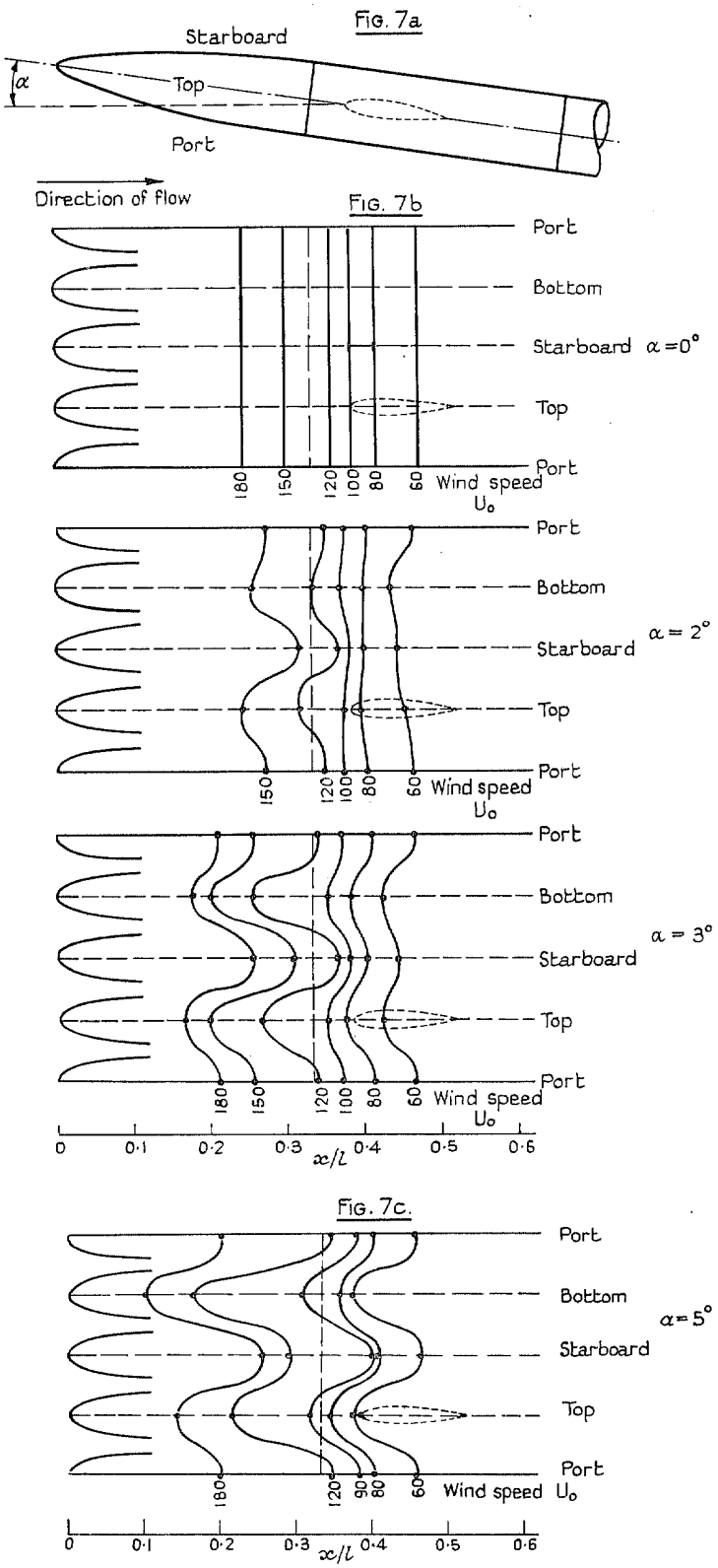

FIGS. 7a to 7c. Diagrams of the developed surface of the body of revolution showing effect of incidence (yaw) on transition.

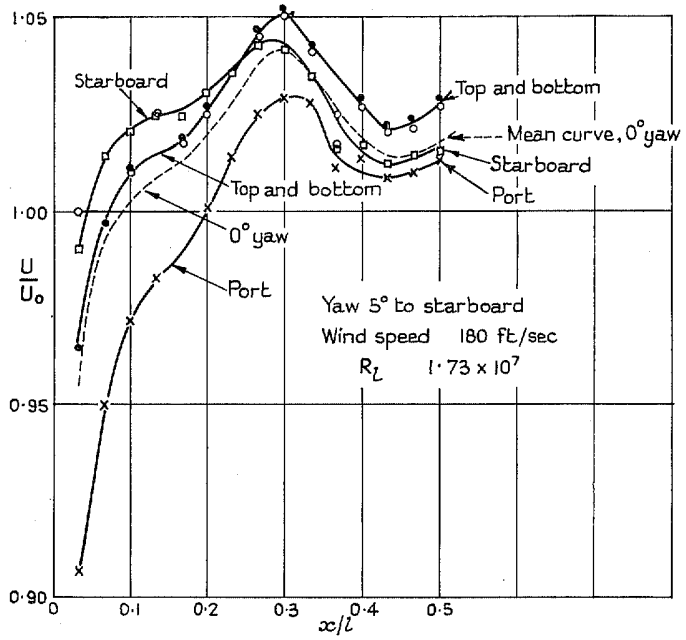

FIG. 8. Effect of incidence (yaw) on velocity distribution.

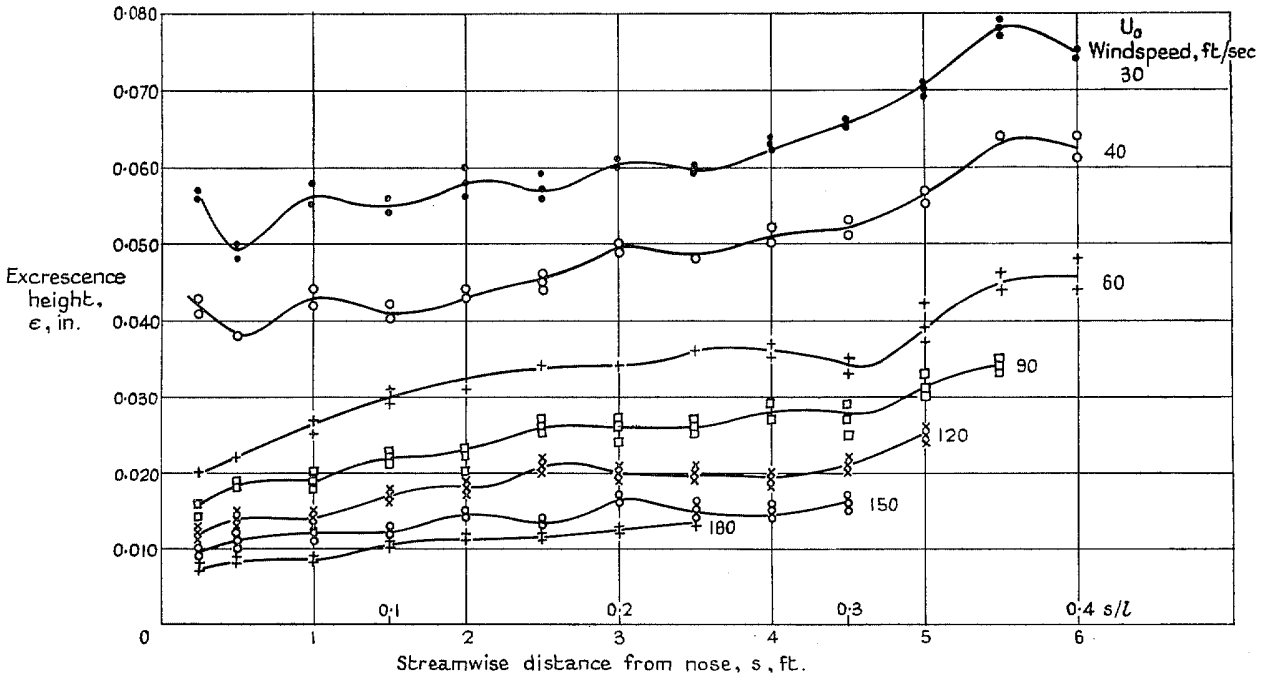

FIG. 9. Variation of critical excrescence height with wind speed and position.

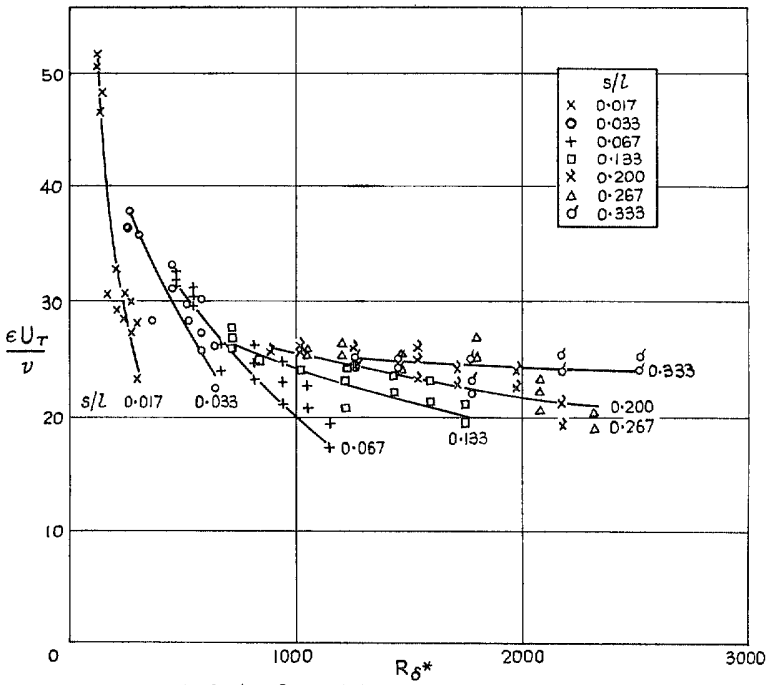

(a) Body of revolution (zero incidence)

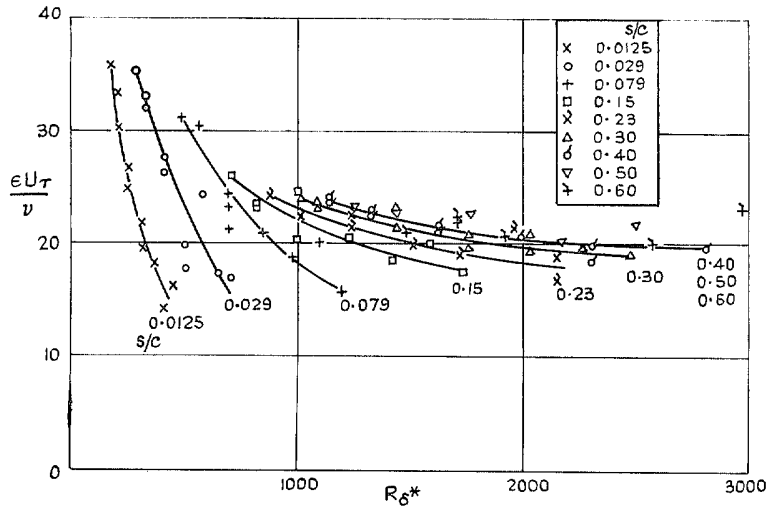

(b) AD-8 aerofoil at 2° incidence

FIGS. 10a and 10b. Variation of $(\varepsilon U_\tau/\nu)_{\text{crit}}$ with boundary-layer Reynolds number.

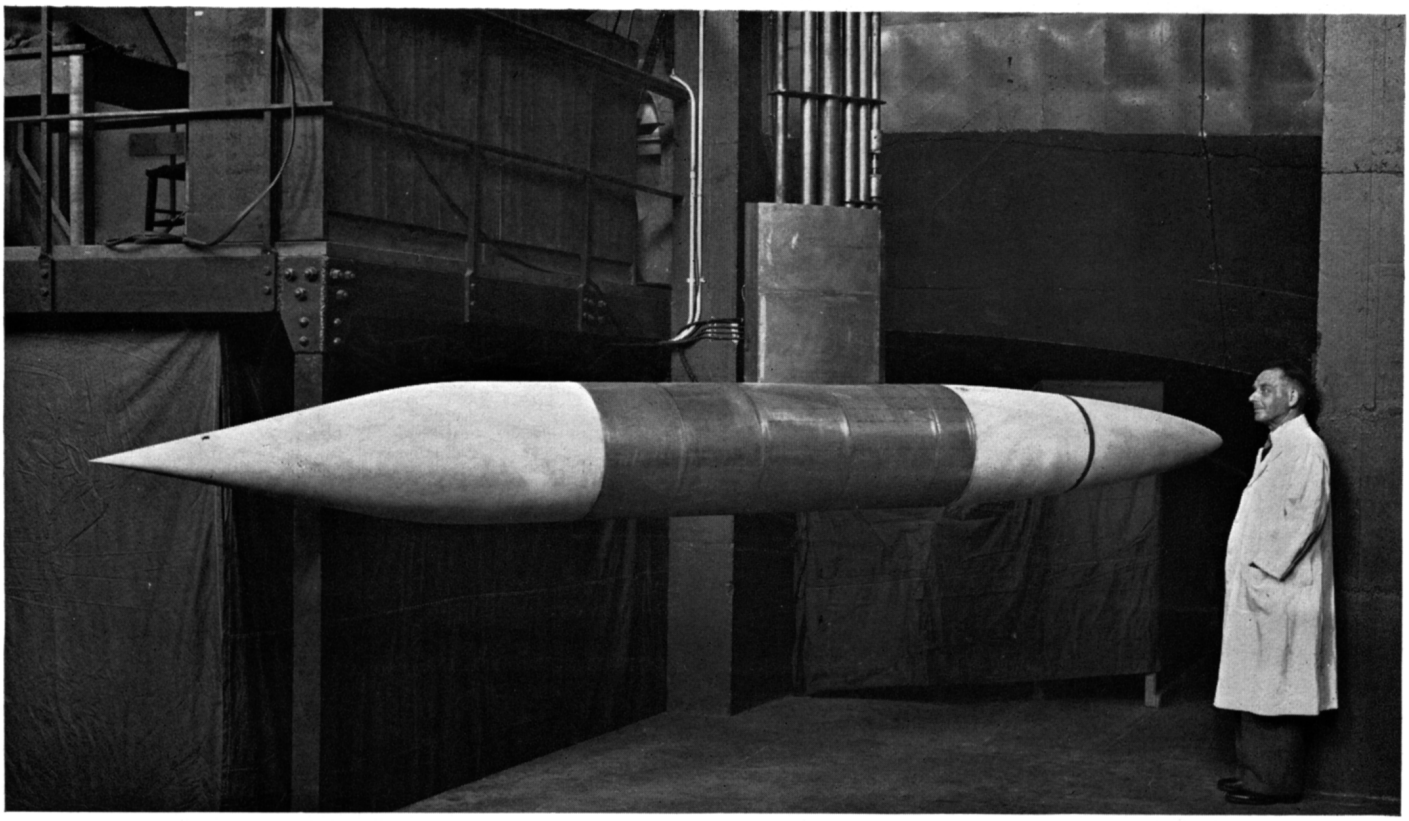

Tail Nose

FIG. 11. Porous body of revolution.

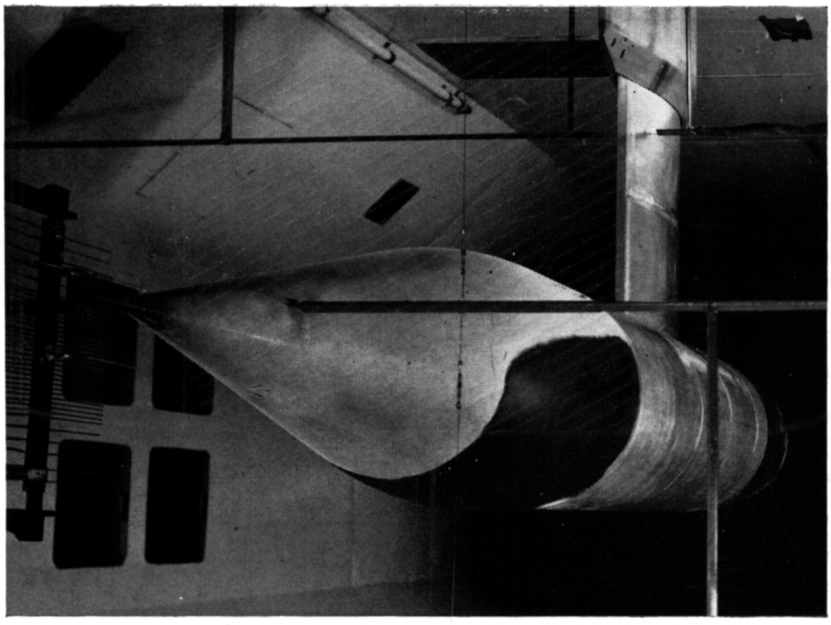

FIG. 12. Porous body in tunnel, showing wake comb and china-clay indication of far-back transition (Tunnel wind speed 80 ft/sec).

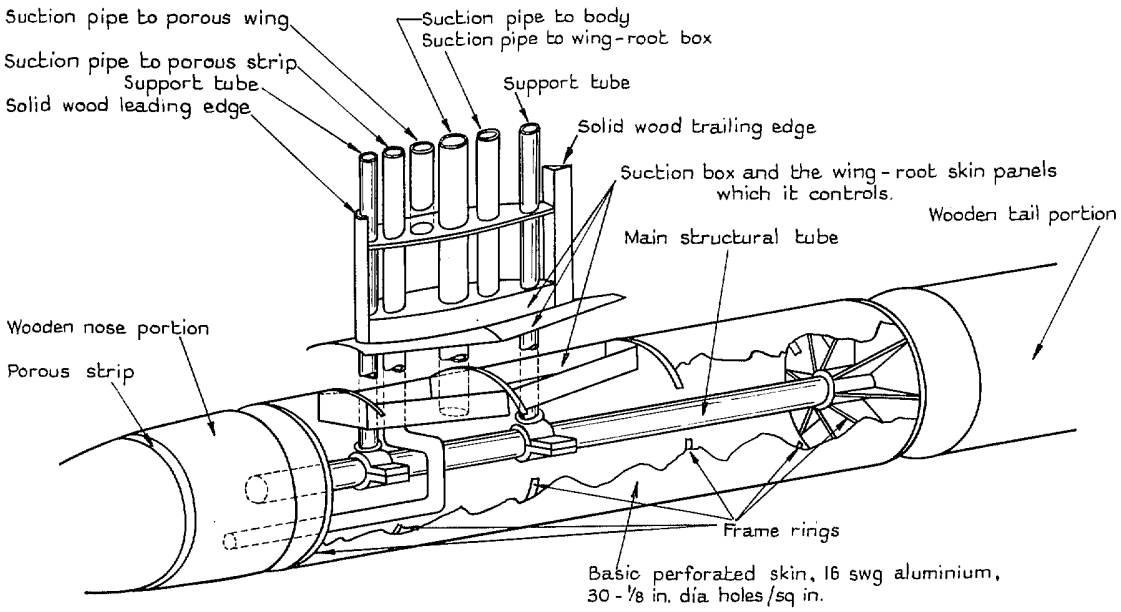

FIG. 13. Basic construction of porous portion of body.

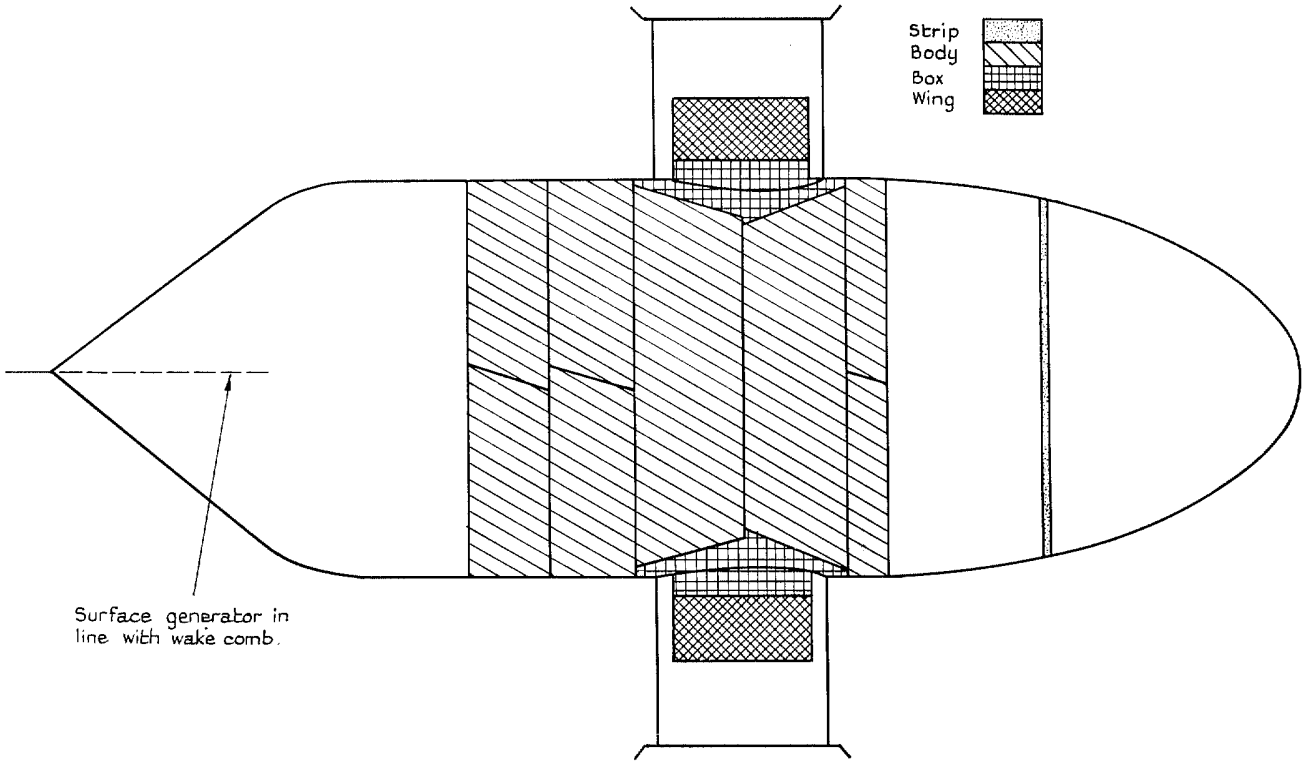

FIG. 14. Development of model surface showing the arrangement of porous-skin panels, location of suction compartments and the alignment of wake comb.

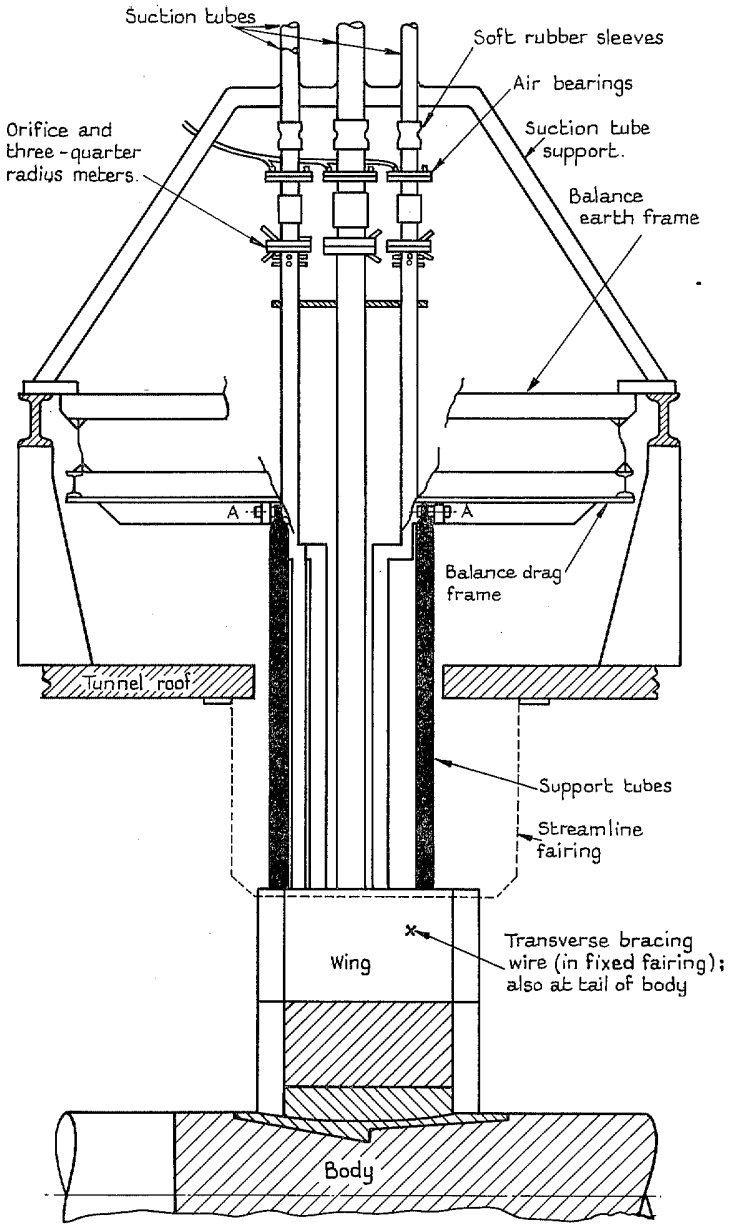

FIG. 15. Suspension of body in tunnel from roof balance.

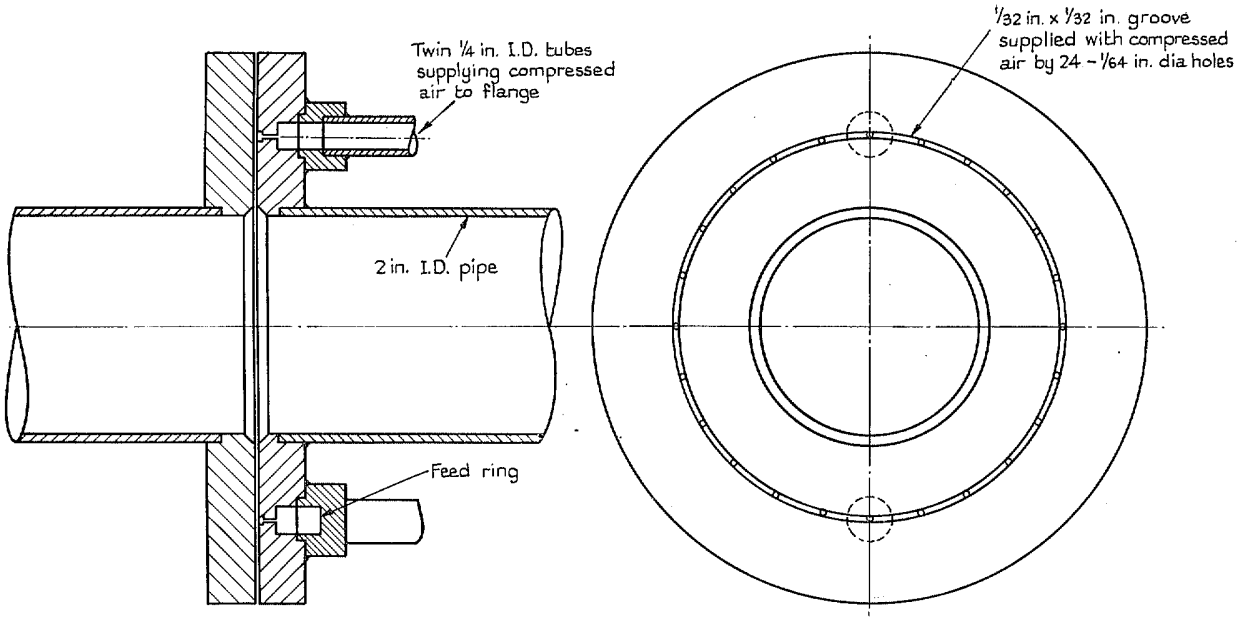

FIG. 16. 'Air-bearing' for suction-pipe connection to model.

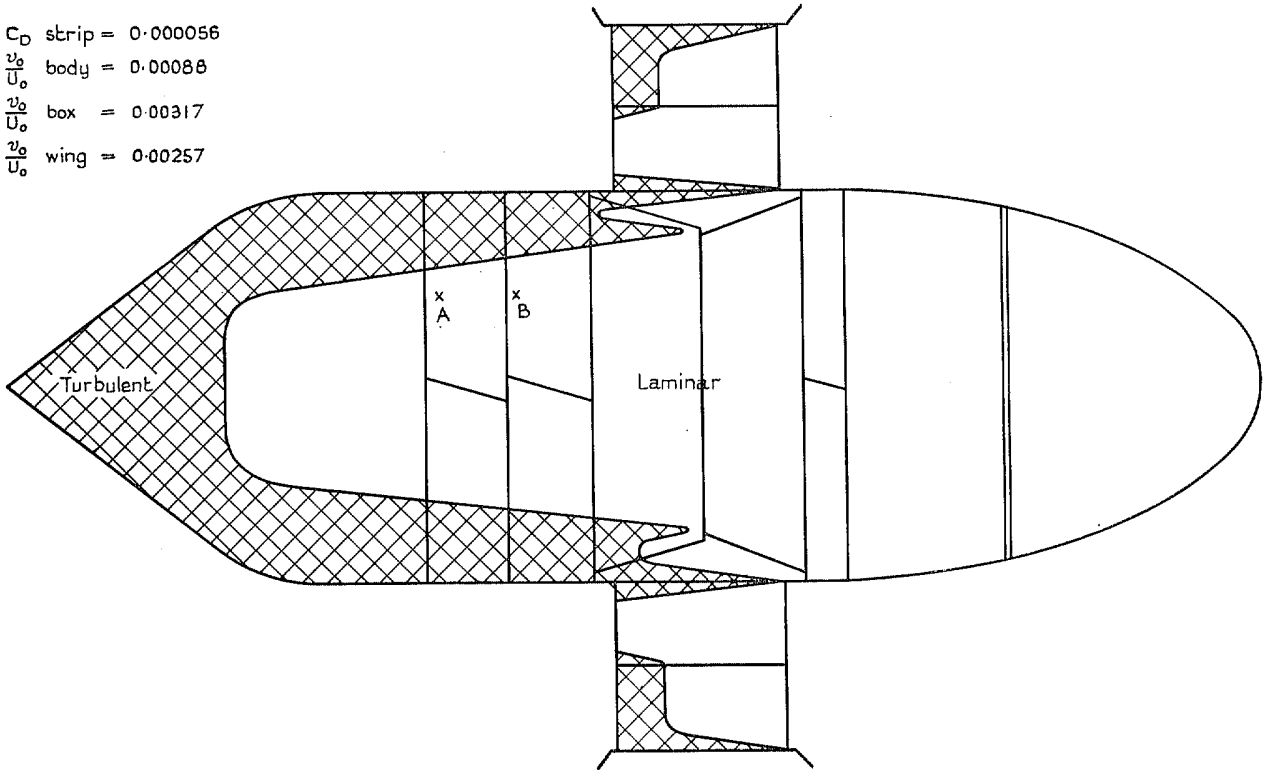

FIG. 17. Transition pattern on model.—Wind speed 80 ft/sec ; Incidence 0 deg.—With suction.

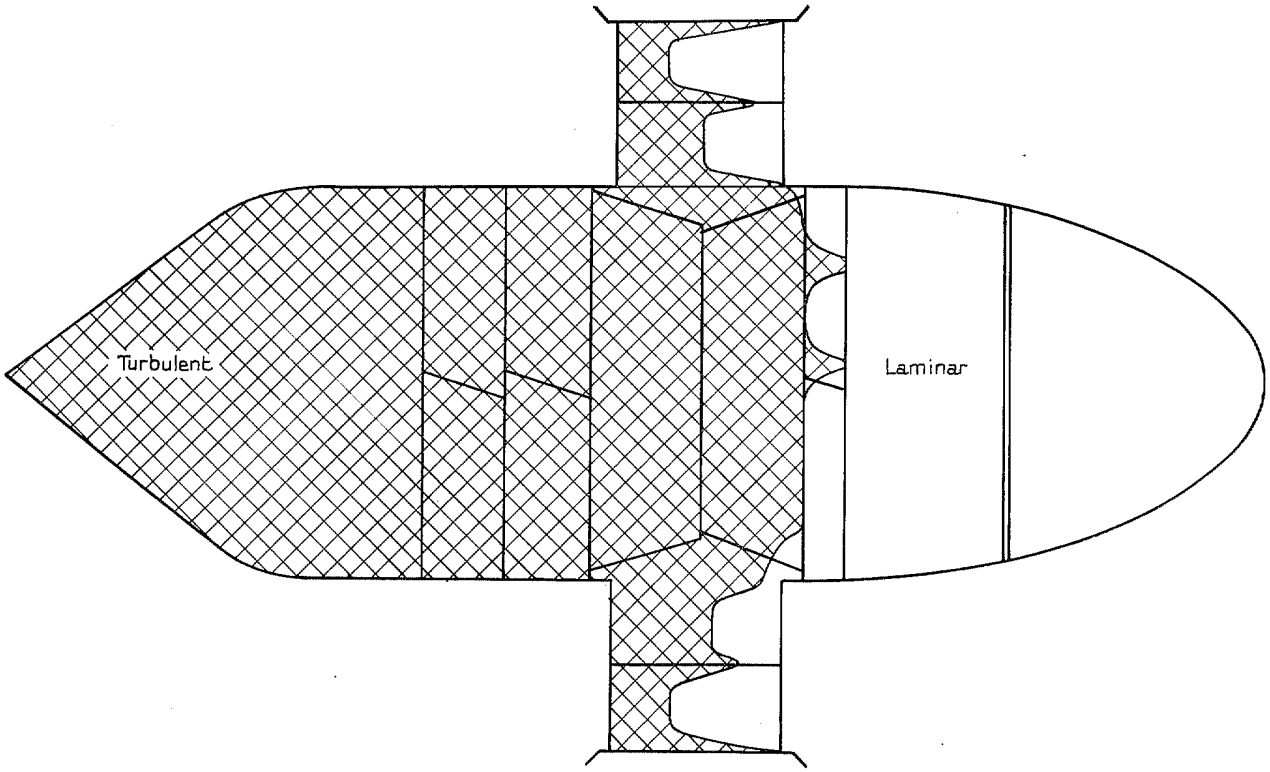

FIG. 18. Transition pattern on model.—Wind speed 80 ft/sec ; Incidence 0 deg.—Zero suction.

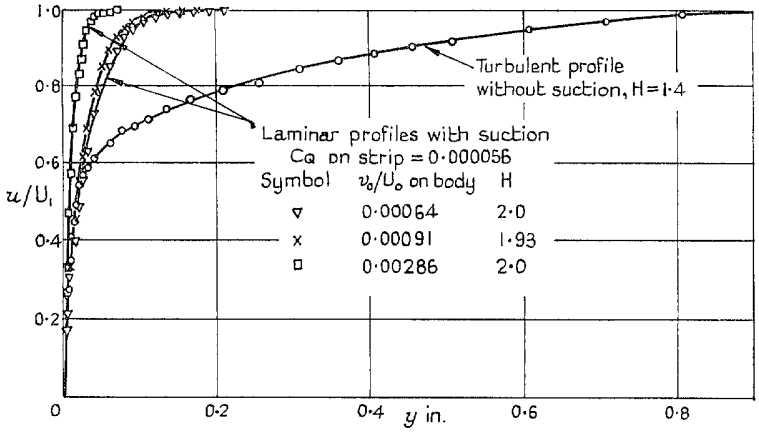

FIG. 19. Velocity profiles at rear of porous surface, 9·86 ft from nose (Position A in Fig. 16).

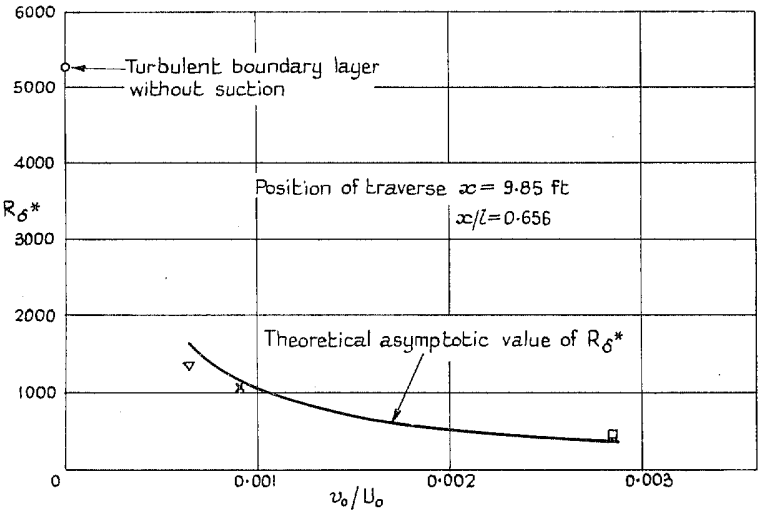

FIG. 20. Variation with suction velocity of the boundary-layer Reynolds number R_δ^* at the rear of the porous surface on the body.

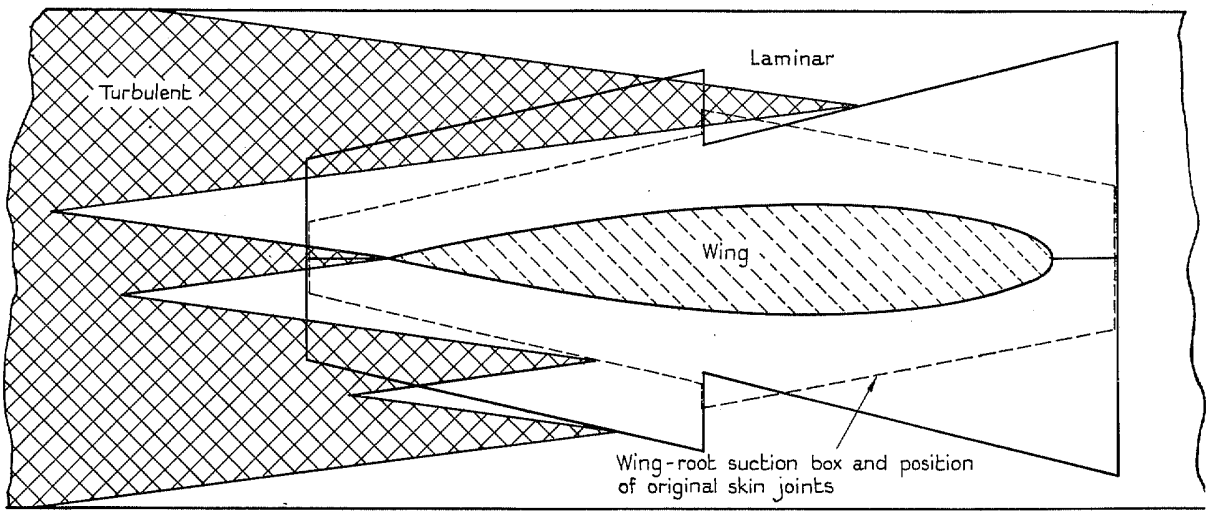

FIG. 21. Plan showing modification to panels around wing root and transition pattern with suction; incidence 0 deg.

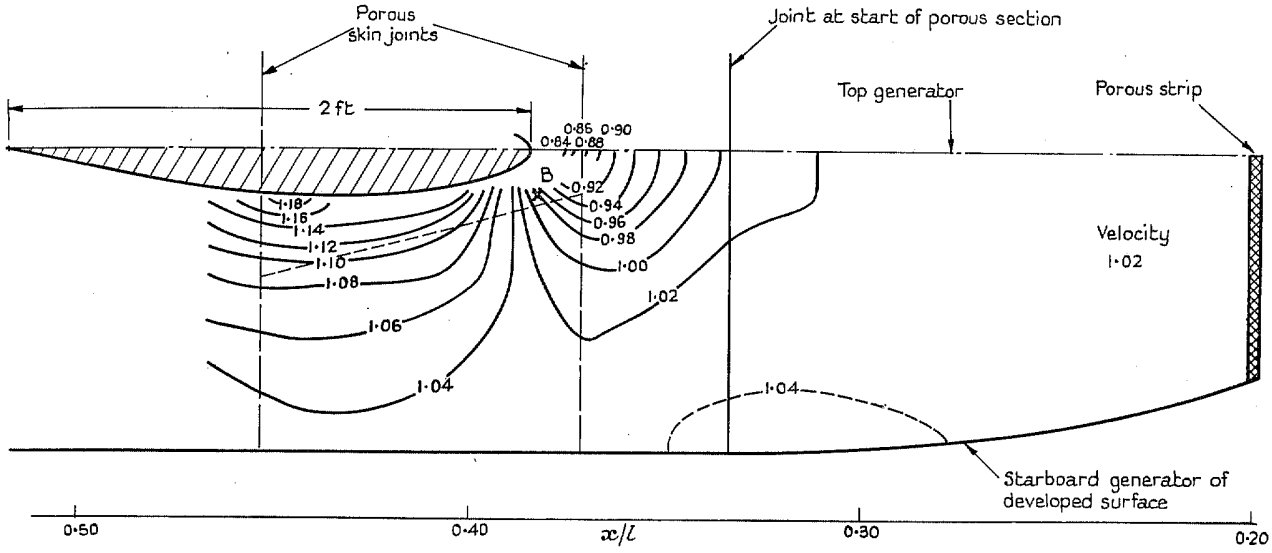

The numbers indicate the magnitude of the velocity outside the boundary layer in terms of the free-stream velocity.

FIG. 22. Isobars on the surface of the body near the wing root.—Zero incidence and yaw.—Wind speed 80 ft/sec.

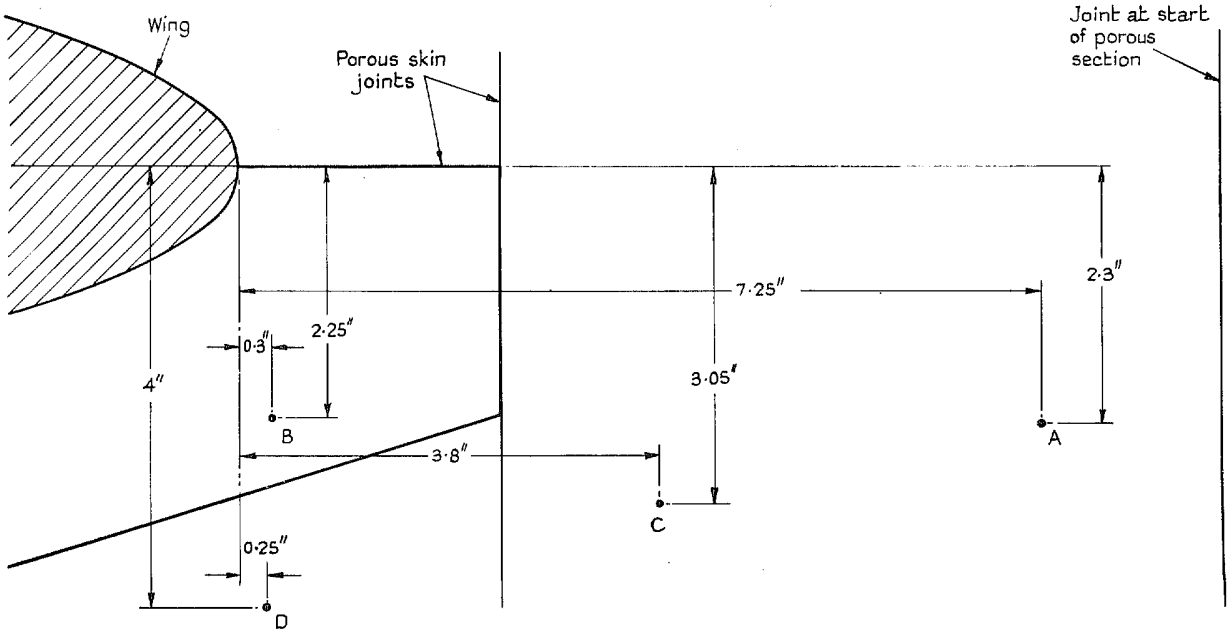

FIG. 23. Sketch showing boundary-layer traverse positions on body near wing root.

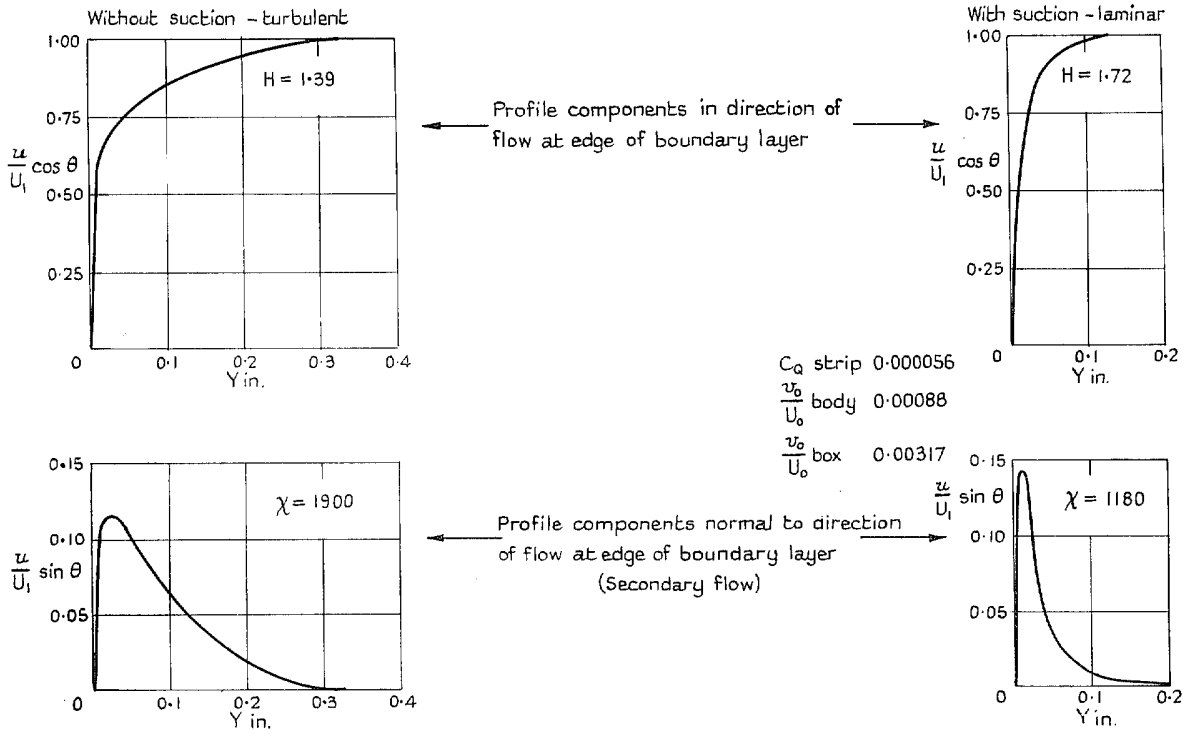

FIG. 24. Effect of suction on secondary flow due to wing-body junction.

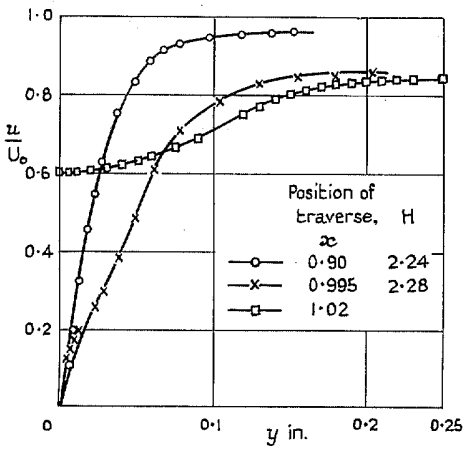

FIG. 25. Boundary-layer profiles at rear of wing. $U_0 = 80$ ft/sec ; $v_0/U_0 = 0{\cdot}00257$.

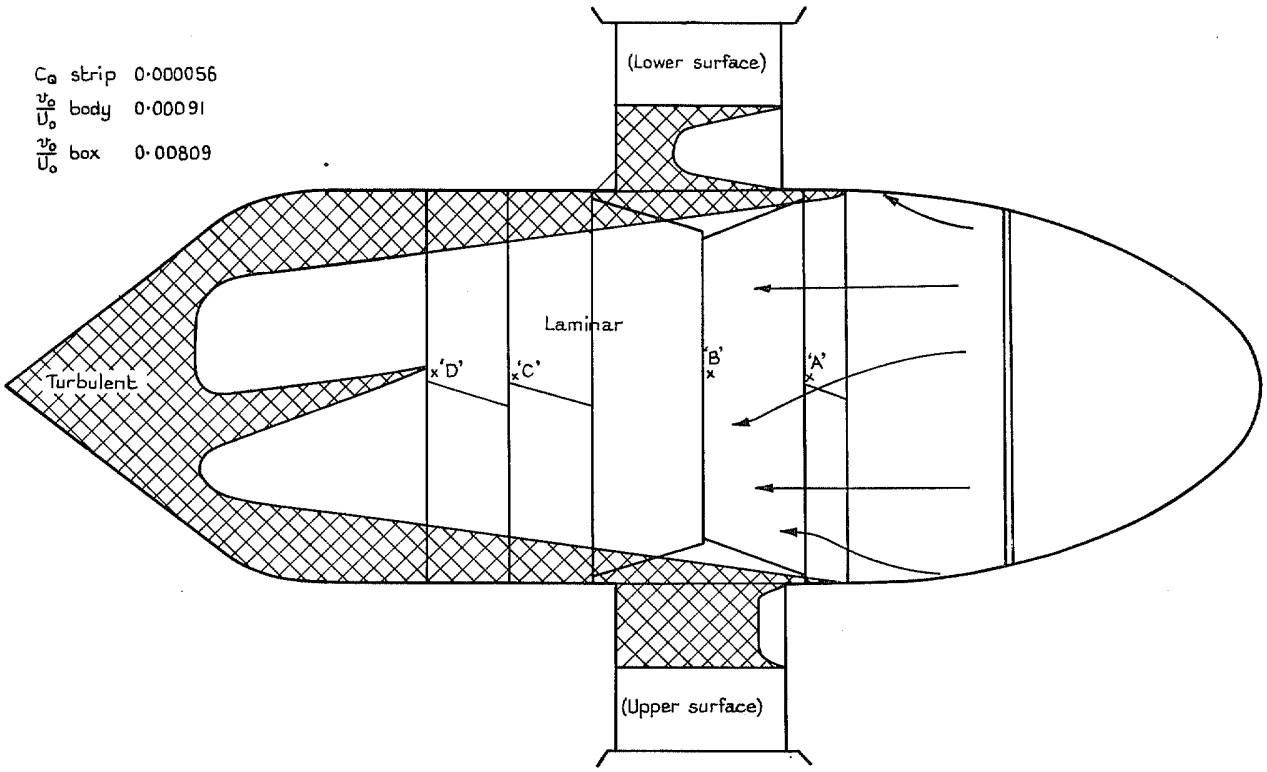

FIG. 26. Transition pattern on model.—Wind speed 80 ft/sec ; yaw 5 deg.—With suction.

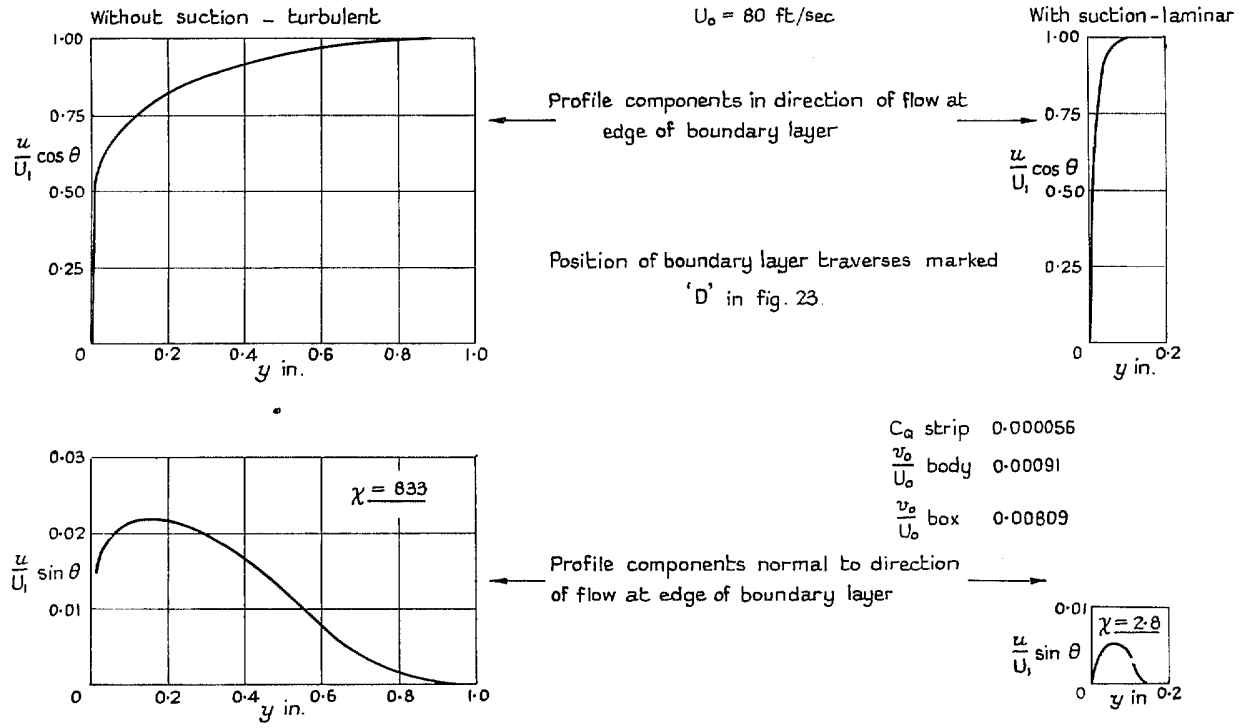

FIG. 27. Effect of suction on secondary flow due to 5-deg yaw.

(78372) Wt. 3523/8210 K.7 6/60 Hw PRINTED IN ENGLAND

Publications of the Aeronautical Research Council

ANNUAL TECHNICAL REPORTS OF THE AERONAUTICAL RESEARCH COUNCIL (BOUND VOLUMES)

1939 Vol. I. Aerodynamics General, Performance, Airscrews, Engines. 50*s.* (52*s.*).
Vol. II. Stability and Control, Flutter and Vibration, Instruments, Structures, Seaplanes, etc. 63*s.* (65*s.*)

1940 Aero and Hydrodynamics, Aerofoils, Airscrews, Engines, Flutter, Icing, Stability and Control, Structures, and a miscellaneous section. 50*s.* (52*s.*)

1941 Aero and Hydrodynamics, Aerofoils, Airscrews, Engines, Flutter, Stability and Control, Structures. 63*s.* (65*s.*)

1942 Vol. I. Aero and Hydrodynamics, Aerofoils, Airscrews, Engines. 75*s.* (77*s.*)
Vol. II. Noise, Parachutes, Stability and Control, Structures, Vibration, Wind Tunnels. 47*s.* 6*d.* (49*s.* 6*d.*)

1943 Vol. I. Aerodynamics, Aerofoils, Airscrews. 80*s.* (82*s.*)
Vol. II. Engines, Flutter, Materials, Parachutes, Performance, Stability and Control, Structures. 90*s.* (92*s.* 9*d.*)

1944 Vol. I. Aero and Hydrodynamics, Aerofoils, Aircraft, Airscrews, Controls. 84*s.* (86*s.* 6*d.*)
Vol. II. Flutter and Vibration, Materials, Miscellaneous, Navigation, Parachutes, Performance, Plates and Panels, Stability, Structures, Test Equipment, Wind Tunnels. 84*s.* (86*s.* 6*d.*)

1945 Vol. I. Aero and Hydrodynamics, Aerofoils. 130*s.* (132*s.* 9*d.*)
Vol. II. Aircraft, Airscrews, Controls. 130*s.* (132*s.* 9*d.*)
Vol. III. Flutter and Vibration, Instruments, Miscellaneous, Parachutes, Plates and Panels, Propulsion. 130*s.* (132*s.* 6*d.*)
Vol. IV. Stability, Structures, Wind Tunnels, Wind Tunnel Technique. 130*s.* (132*s.* 6*d.*)

Annual Reports of the Aeronautical Research Council—

1937 2*s.* (2*s.* 2*d.*) 1938 1*s.* 6*d.* (1*s.* 8*d.*) 1939–48 3*s.* (3*s.* 5*d.*)

Index to all Reports and Memoranda published in the Annual Technical Reports, and separately—

April, 1950 - - - - R. & M. 2600 2*s.* 6*d.* (2*s.* 10*d.*)

Author Index to all Reports and Memoranda of the Aeronautical Research Council—

1909—January, 1954 R. & M. No. 2570 15*s.* (15*s.* 8*d.*)

Indexes to the Technical Reports of the Aeronautical Research Council—

December 1, 1936—June 30, 1939	R. & M. No. 1850	1*s.* 3*d.* (1*s.* 5*d.*)
July 1, 1939—June 30, 1945	R. & M. No. 1950	1*s.* (1*s.* 2*d.*)
July 1, 1945—June 30, 1946	R. & M. No. 2050	1*s.* (1*s.* 2*d.*)
July 1, 1946—December 31, 1946	R. & M. No. 2150	1*s.* 3*d.* (1*s.* 5*d.*)
January 1, 1947—June 30, 1947	R. & M. No. 2250	1*s.* 3*d.* (1*s.* 5*d.*)

Published Reports and Memoranda of the Aeronautical Research Council—

Between Nos. 2251–2349	R. & M. No. 2350	1*s.* 9*d.* (1*s.* 11*d.*)
Between Nos. 2351–2449	R. & M. No. 2450	2*s.* (2*s.* 2*d.*)
Between Nos. 2451–2549	R. & M. No. 2550	2*s.* 6*d.* (2*s.* 10*d.*)
Between Nos. 2551–2649	R. & M. No. 2650	2*s.* 6*d.* (2*s.* 10*d.*)
Between Nos. 2651–2749	R. & M. No. 2750	2*s.* 6*d.* (2*s.* 10*d.*)

Prices in brackets include postage

HER MAJESTY'S STATIONERY OFFICE

York House, Kingsway, London W.C.2; 423 Oxford Street, London W.1; 13a Castle Street, Edinburgh 2; 39 King Street, Manchester 2; 2 Edmund Street, Birmingham 3; 109 St. Mary Street, Cardiff; Tower Lane, Bristol 1; 80 Chichester Street, Belfast, *or through any bookseller.*

S.O. Code No. 23-3145